de Haas-van Alphen effect

Masatsugu Sei Suzuki
Department of Physics, SUNY at Binghamton
(Date: March 30, 2013)

Notations:

$\hbar$:	Planck constant
c:	velocity of the light
$-e$:	charge of electron
m:	mass of free electron
m_c:	cyclotron mass
m:	mass of electron (in theory)
ω_c:	cyclotron frequency ($\omega_c = eB/(m_c c)$)
μ_B	Bohr magneton ($\mu_B = e\hbar/(2m_0 c)$)
Φ_0:	quantum fluxoid ($\Phi_0 = 2\pi\hbar c/2e = 2.0678\times 10^{-7}$ Gauss cm^2)
B:	magnetic field
l:	magnetic length ($l = \sqrt{c\hbar/eB}$)
T:	Tesla (1 T = 10^4 Oe)
Oe	unit of the magnetic field (= Gauss)
ε_F:	the Fermi energy
S_e:	extremal cross-sectional area of the Fermi surface in a plane normal to the magnetic field.

Lev Davidovich Landau (Russian: Ле́в Дави́дович Ланда́у; January 22, 1908– April 1, 1968) was a prominent Soviet physicist who made fundamental contributions to many areas of theoretical physics. His accomplishments include the independent co-discovery of the density matrix method in quantum mechanics (alongside John von Neumann), the quantum mechanical theory of diamagnetism, the theory of superfluidity, the theory of second-order phase transitions, the Ginzburg–Landau theory of superconductivity, the theory of Fermi liquid, the explanation of Landau damping in plasma physics, the Landau pole in quantum electrodynamics, and the two-component theory of neutrinos. He received the 1962 Nobel Prize in Physics for his development of a mathematical theory of superfluidity that accounts for the properties of liquid helium II at a temperature below 2.17°K.

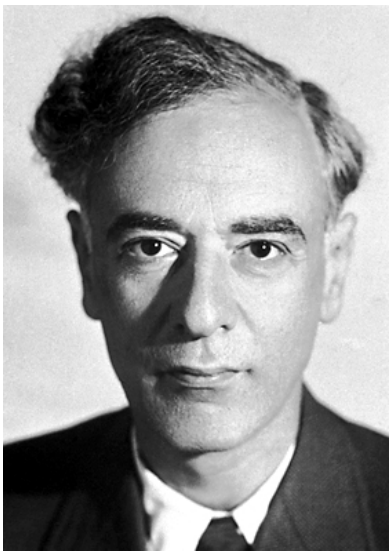

http://en.wikipedia.org/wiki/Lev_Landau

Lars Onsager (November 27, 1903 – October 5, 1976) was a Norwegian-born American physical chemist and theoretical physicist, winner of the 1968 Nobel Prize in Chemistry. He held the Gibbs Professorship of Theoretical Chemistry at Yale University.

After World War II, Onsager researched new topics of interest. He proposed a theoretical explanation of the superfluid properties of liquid helium in 1949; two years later the physicist Richard Feynman independently proposed the same theory. He also worked on the theories of liquid crystals and the electrical properties of ice. While on a Fulbright scholarship to Cambridge University, he worked on the magnetic properties of metals. He developed important ideas on the quantization of magnetic flux in metals. He was awarded the Lorentz Medal in 1958 and the Nobel Prize in Chemistry in 1968.

http://en.wikipedia.org/wiki/Lars_Onsager

1. Introduction

The de Haas-van Alphen (dHvA) effect is an oscillatory variation of the diamagnetic susceptibility as a function of a magnetic field strength (B). The method provides details of the extremal areas of a Fermi surface. The first experimental observation of this behavior was made by de Haas and van Alphen (1930). They have measured a magnetization M of semimetal bismuth (Bi) as a function of the magnetic field (B) in high fields at 14.2 K and found that the magnetic susceptibility M/B is a periodic function of the reciprocal of the magnetic field ($1/B$). This phenomenon is observed only at low temperatures and high magnetic fields. Similar oscillatory behavior has been also observed in magnetoresistance (so called the Shubnikov-de Haas effect).

The dHvA phenomenon was explained by Landau[1] as a direct consequence of the quantization of closed electronic orbits in a magnetic field and thus as a direct observational manifestation of a purely quantum mechanics. The phenomenon became of even greater interest and importance when Onsager[2] pointed out that the change in $1/B$ through a single period of oscillation was determined by the remarkably simple relation,

$$P = \frac{1}{F} = \Delta(\frac{1}{B}) = \frac{2\pi e}{\hbar c}\frac{1}{S_e}, \qquad (1)$$

where P is the period (Gauss^{-1}) of the dHvA oscillation in $1/B$, F is the dHvA frequency (Gauss), and S_e is any extremal cross-sectional area of the Fermi surface in a plane normal to the magnetic field. If the z axis is taken along the magnetic field, then the are of a Fermi surface cross section at height k_z is $S(k_z)$ and the extremal areas S_e are the values of $S(k_z)$ at the k_z where $dS(k_z)/dk_z = 0$. Thus maximum and minimum cross sections are among the extremal ones. Since altering the magnetic field direction brings different

extremal areas into play, all extremal areas of the Fermi surface can be mapped out. When there are two extremal cross-sectional area of the Fermi surface in a plane normal to the magnetic field and these two periods are nearly equal, a beat phenomenon of the two periods will be observed from which each period must be disentangled through the analysis of the Fourier transform.

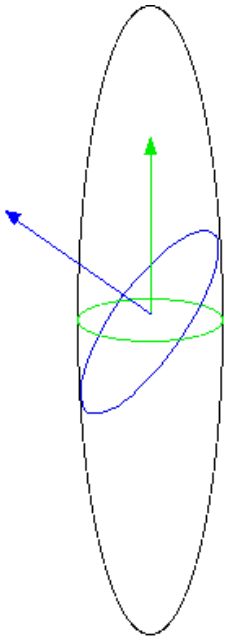

Fig.1 Fermi surface of the hole pocket for Bi. The magnetic field (denoted by arrows) is in the *YZ* plane.

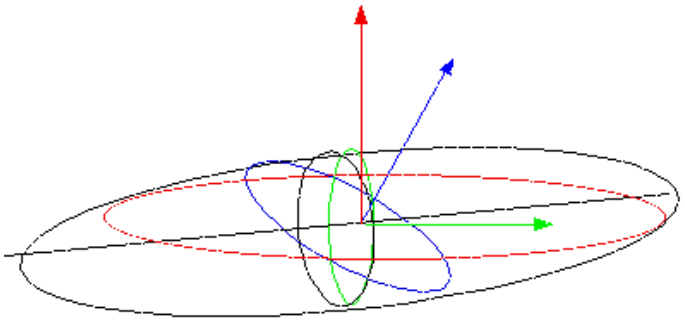

Fig.2 Fermi surface of the electron (*a*) pocket for Bi. The major axis of the ellipsoid is tilted by 6.5° from the bisectrix axis.

Experimentally the value of S_e (cm^{-2}) can be determined from more convenient form

$$S_e = \frac{2\pi e}{\hbar c P} = \frac{2\pi^2}{\Phi_0}\frac{1}{P} = 9.54592\times 10^7 \ (\text{Gauss}^{-1}\ \text{cm}^{-2})/P(\text{Gauss}^{-1})\ [\text{cm}^{-2}] \qquad (2)$$

where P is in unit of Gauss^{-1} and Φ_0 (= $2\pi\hbar c/2e = 2.0678\times 10^{-7}$ Gauss cm^2) is the quantum fluxoid.

The dHVA effect can be observed in very pure metals only at low temperatures and in strong magnetic fields that satisfy

$$\varepsilon_F >> \hbar\omega_c >> k_B T\,. \qquad (3)$$

The first inequality means that the electron system is quantum-mechanically degenerate even though, as required by the second inequality, the magnetic field is sufficiently strong. On the other hand, the observation of dHvA oscillation is determined by

$$\frac{\Delta H}{H} \approx \frac{\hbar\omega_c}{\varepsilon_F} \approx 10^{-4}. \tag{4}$$

That is, for the observation of oscillations, the fluctuations ΔH in an magnetic field should be small and the electron density should not be too high because the period depends on the ratio $\hbar\omega_c / \varepsilon_F$.

2. Fermi surface of Bi[3-10]

2.1 Energy dispersion relation

Bismuth is a typical semimetal. The model of the band structure of Bi consists of a set of three equivalent electron ellipsoids at the L point and a single hole ellipsoid at the T point (see the Brillouin zone in Sec 2.2). In one of the electron ellipsoids (a-pocket), the energy E is related to the momentum $\boldsymbol{p}$ in the absence of a magnetic field by

$$E(1+\frac{E}{E_G}) = \frac{1}{2m_0}\boldsymbol{p}\cdot\boldsymbol{m}^{*-1}\cdot\boldsymbol{p}, \tag{5}$$

(Lax model[5] or ellipsoidal non-parabolic model) where E_G is the energy gap to the next lower band and $\boldsymbol{m}^*$ is the effective mass tensor in units of the free electron mass m_0. The effective mass tensor $\boldsymbol{m}_a^*$ is of the form

$$\boldsymbol{m}_a^* = \begin{pmatrix} m_1 & 0 & 0 \\ 0 & m_2 & m_4 \\ 0 & m_4 & m_3 \end{pmatrix}, \tag{6}$$

where 1, 2, and 3 refer to the binary (X), the bisectrix (Y), and the trigonal (Z) axes, respectively. The other two electron ellipsoids (b and c pockets) are obtained by rotations of ±120° about the trigonal axis, respectively. The effective mass tensors $\boldsymbol{m}_b^*$ for the b pocket and $\boldsymbol{m}_c^*$ for the c pocket are given by

$$\boldsymbol{m}_{b,c}^* = \begin{pmatrix} \frac{m_1+3m_2}{4} & \pm\frac{\sqrt{3}(m_1-m_2)}{4} & \pm\frac{\sqrt{3}m_4}{2} \\ \pm\frac{\sqrt{3}(m_1-m_2)}{4} & \frac{3m_1+m_2}{4} & \frac{-m_4}{2} \\ \pm\frac{\sqrt{3}m_4}{2} & \frac{-m_4}{2} & m_3 \end{pmatrix}. \tag{7}$$

For the holes, the energy momentum relationship in the absence of a magnetic field is taken to be

$$E_0 - E = \frac{1}{2m_0} \boldsymbol{p} \cdot \boldsymbol{M}^{*-1} \cdot \boldsymbol{p} \,, \tag{8}$$

where E_0 is the energy of the top of the hole band relative to the bottom of the electron band and the effective mass tensor $\boldsymbol{M}^*$ for the hole pocket is

$$\boldsymbol{M}^* = \begin{pmatrix} M & 0 & 0 \\ 0 & M_1 & 0 \\ 0 & 0 & M_3 \end{pmatrix}. \tag{9}$$

The Fermi surface consists of one hole ellipsoid of revolution and three electron ellipsoids. One electron ellipsoid has its major axis tilted by a small positive angle (= 6.5º) from the bisectrix direction..

Table I Bi band parameters used by Takano and Kawamura[8]

Mass parameter	m_1	m_2	m_3	m_4	M_1	M_3
At Fermi level	0.0071	1.50	0.0301	0.170	0.067	0.76
At the band edge	0.0016	0.342	0.0068	0.038	0.048	0.54

Carrier density (H=0)	N=2.85×10^{17} cm^{-3}
Fermi energy (H=0)	E_F=25.4 meV
Overlap energy (H=0)	E_o=37.6 meV
Band gap	E_g=15 meV[27]
	E_{gh}=60 meV[16]

Spin-splitting factor γ[12]	Electrons A	Holes
H//binary axis	0.356	0.14
H//trigonal axis	0.59	1.94

2.2 Brillouin zone and Fermi surface of Bi

The Brillouin zone and the Fermi surface of Bi are shown here.

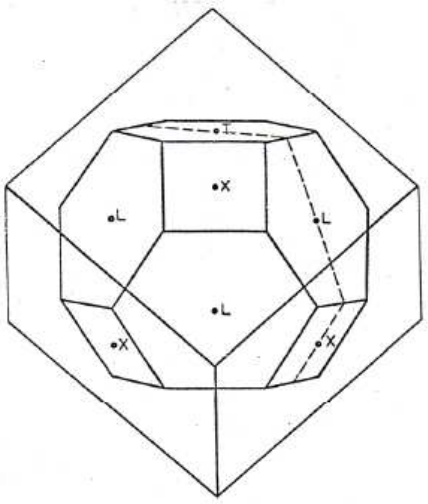

Fig.3 Brillouin zone of bismuth[3-10]

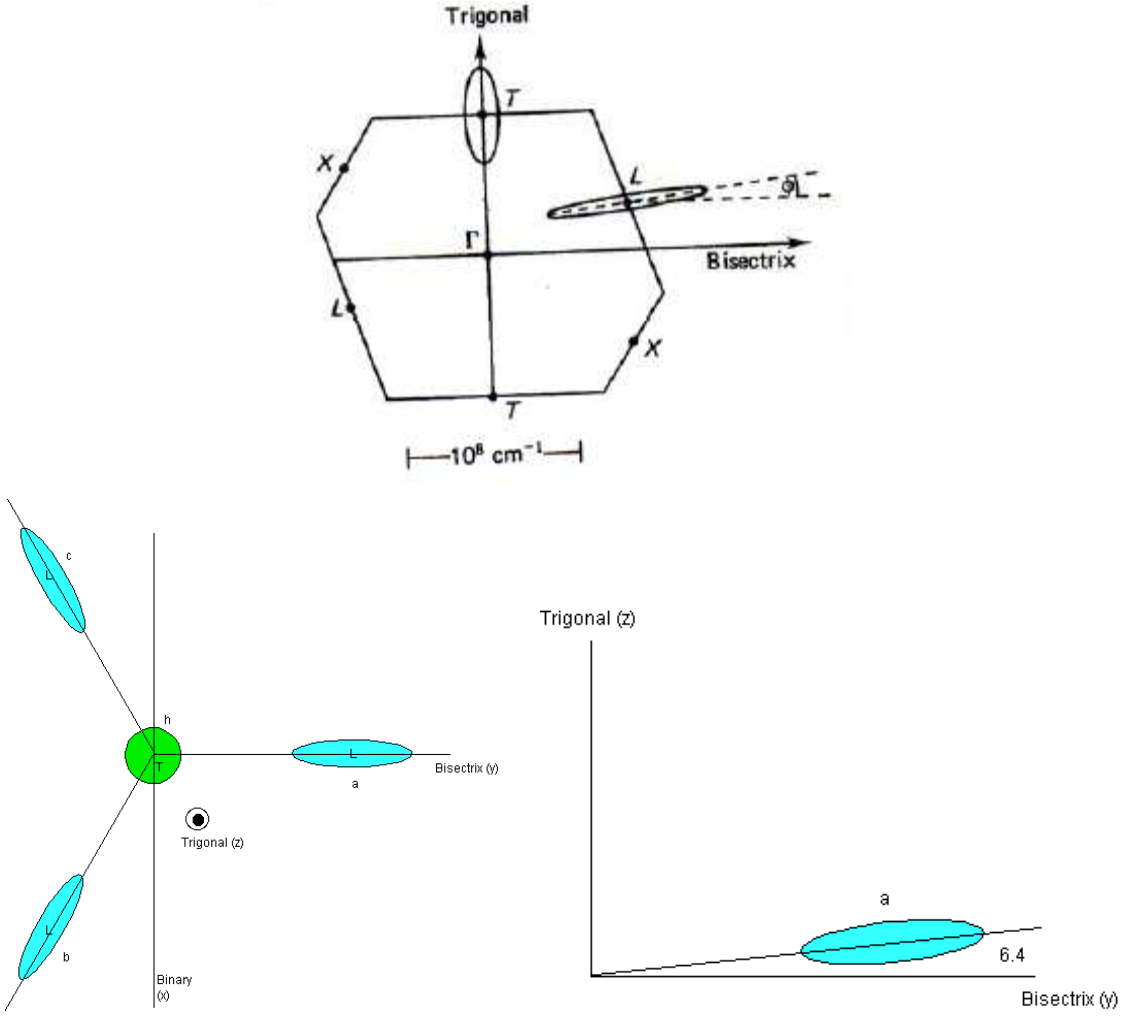

Fig.4 Fermi surface of bismuth: binary axis (*X*), bisectrix (*Y*), and trigonal (*Z*). *a*, *b*, *c* are the electron pocket (Fermi surfaces) and *h* is the hole pocket.

3. Techniques for the measurement of dHvA

There are two major techniques to measure the dHvA oscillations: (1) field modulation method using a lock-in amplifier. (2) torque method. Because of the Fermi surface in Bi is so small, the dHvA effect can be observed in quite small fields as low as 100 Oe at 0.3 K) and at fairly high temperatures up to 20 or 30 K at fields of a few kOe). It is in fact the metal in which the dHvA effect was first discovered and have probably been more studied ever since than any other metal.

3.1 Field modulation method

The system consists of a detecting coil, a compensation coil, and a filed modulation coil. The static magnetic field B (superconducting magnet or ion core magnet) is modulated by a small AC field $h_0 \cos \omega t$ (ω is a angular frequency) generated by the field modulation coil. The direction of the AC filed is parallel to that of a static magnetic field B. The voltage induced in the pick-up coil is given by

$$v \propto \omega\{h\frac{\partial M}{\partial h}\sin(\omega t) + \frac{1}{2}h^2 \sin(2\omega t)\frac{\partial^2 M}{\partial h^2} + ...\}, \qquad (10)$$

where $h << B$. The signal obtained from the pick-up coil was phase sensitively detected at the first harmonic or second harmonic modes with a lock-in amplifier. The DC signal is proportional to $\omega h\frac{\partial M}{\partial h}$ for the first-harmonic mode and $\omega h^2 \frac{\partial^2 M}{\partial h^2}$ for the second-harmonic mode. These signals are periodic in $1/B$. The Fourier analysis leads to the dHvA frequency F (or the dHvA period $P = 1/F$).

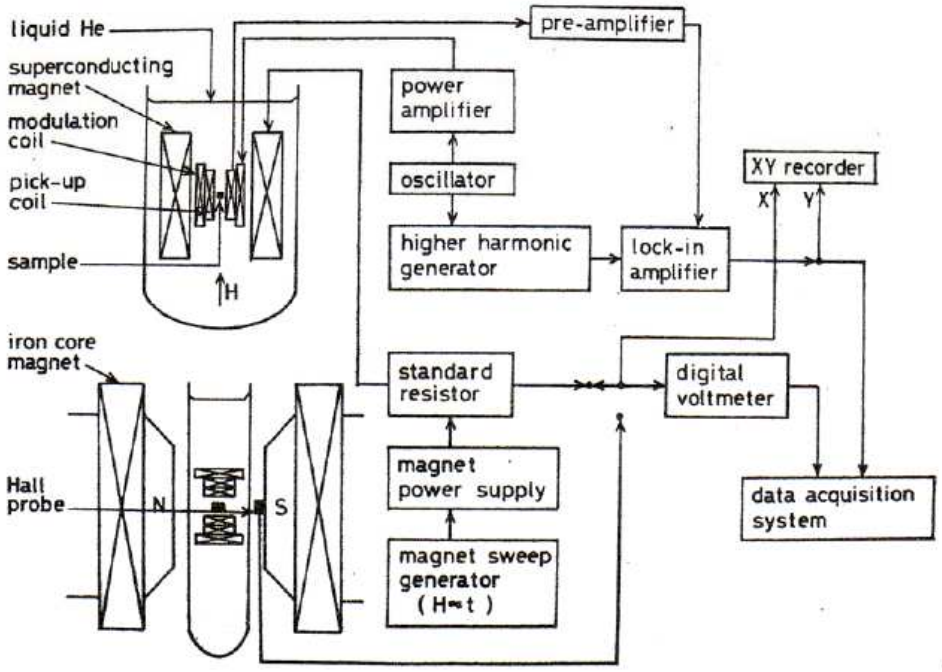

Fig.5 The block diagram of the apparatus for the measurement of the dHvA effect by means of the field modulation method.[10]

3.2 Torque method

When an external magnetic field is applied to the sample, there is a torque on the sample, given $M_{\perp}BV$, where $M_{\perp}$ is the component of $\boldsymbol{M}$ perpendicular to $\boldsymbol{B}$ and V is the volume. Using this method, the absolute value of the magnetization can be exactly determined. Note that the torque is equal to zero when the direction of the magnetic filed is parallel to the symmetric direction of the sample.

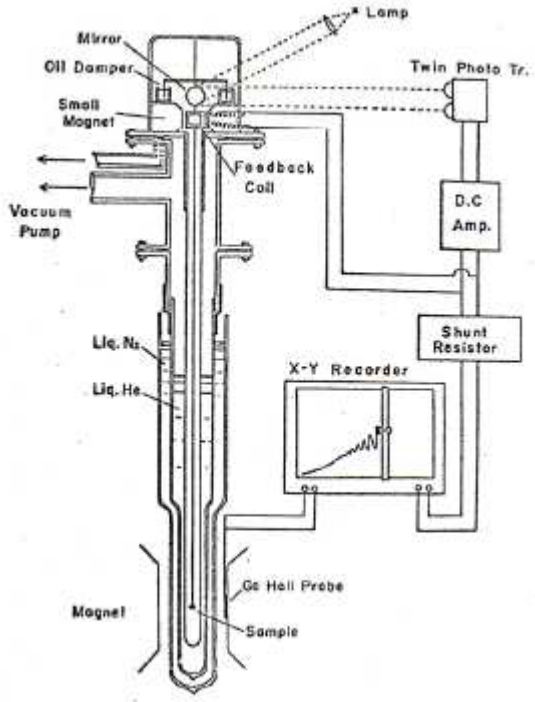

Fig.6 The block diagram of the apparatus for measuring the dHvA effect by Torque de Haas method.[9]

4. Results of dHvA effect in Bi

4.1 Result from the modulation method (Suzuki[9])

We show typical examples of the dHvA effect in Bi and the Fourier spectra for the dH vH periods.

Fig.2 Fermi surface of the electron (*a*) pocket for Bi. The major axis of the ellipsoid is tilted by 6.5º from the bisectrix axis.

(a) (b)

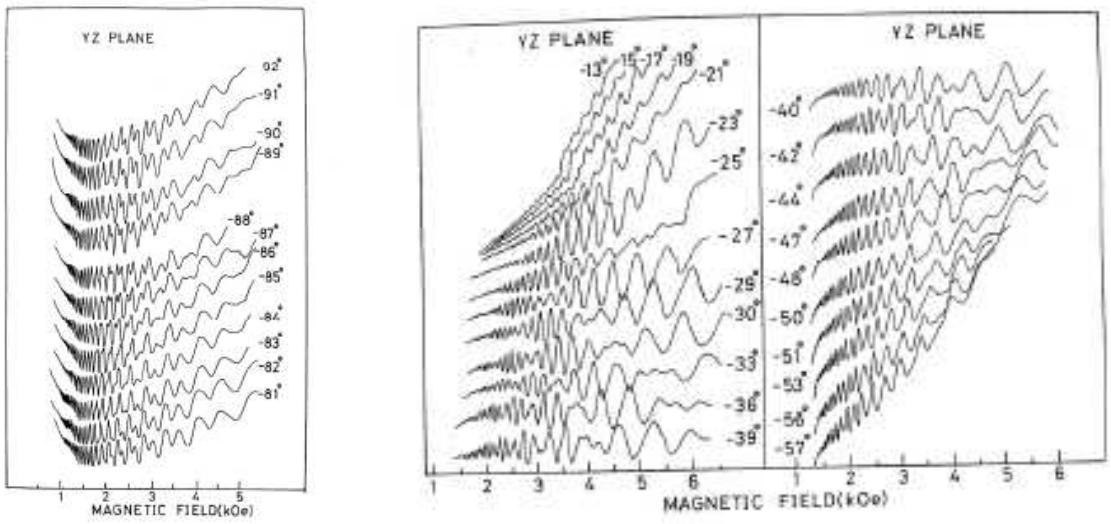

Fig.7 The dHvA effect of Bi in the YZ plane. T = 1.5 K. This signal corresponds to the first harmonics ($\partial M / \partial h$).

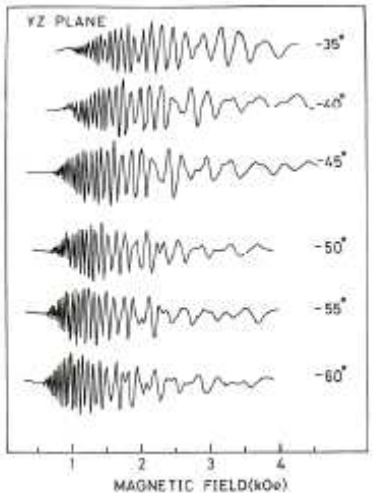

Fig.8 The dHvA effect of Bi in the YZ plane. T = 1.5 K. The signal corresponds to the second harmonics ($\partial^2 M / \partial h^2$).

4.2 Result of torque de Haas (Suzuki[9])

We show typical examples of the torque de Haas in Bi.

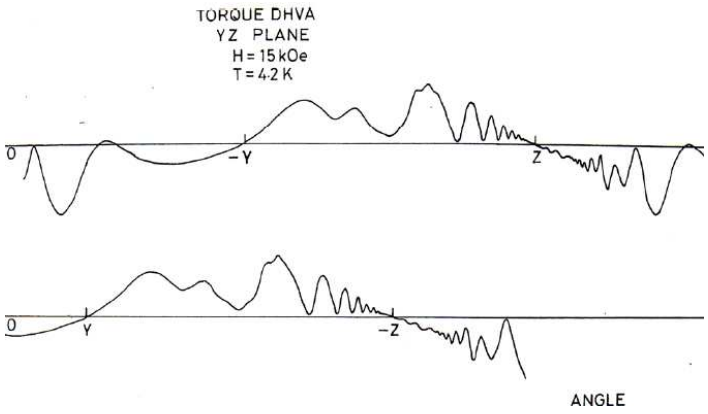

Fig.9 Angular dependence of the torque de Has in the *YZ* plane. The torque is zero at the symmetry axes (*Y* and *Z*). $B = 15$ kOe. $T = 4.2$ K.

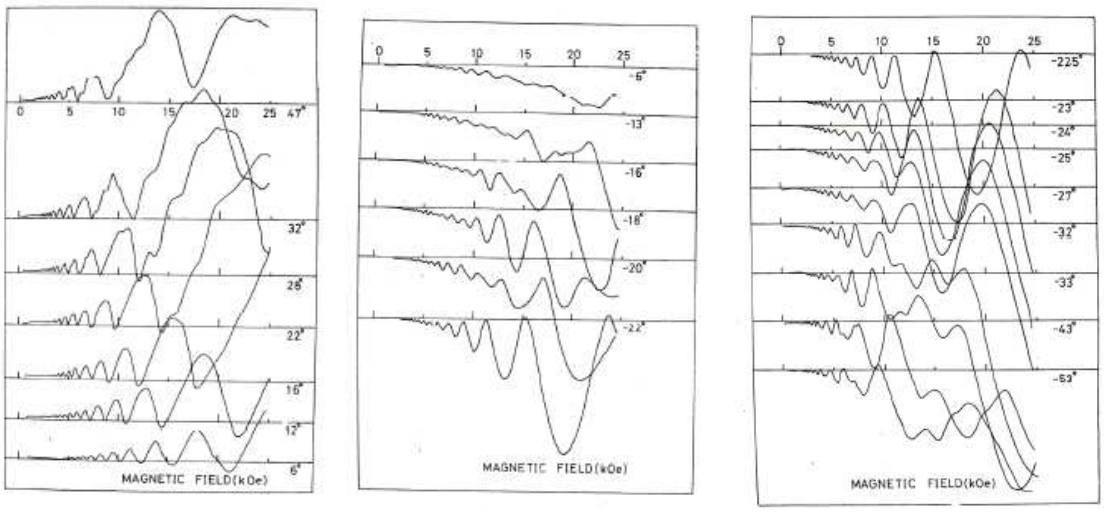

Fig.10 The torque de Haas in the YZ plane. $T = 1.5$ K.

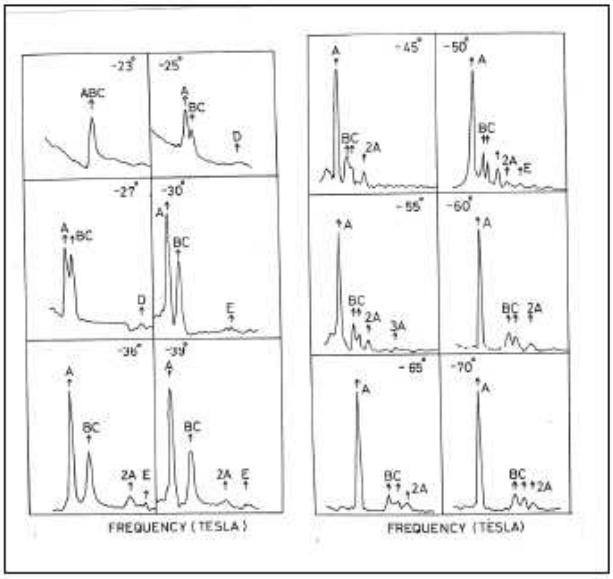

Fig.11 The Fourier spectrum of the dHvA oscillation. The magnetic field is oriented s in the YZ plane. The *Z* axis corresponds to 0º. The branches A, B, and C correspond to the *a*-, *b*-, and *c*-electron pockets, respectively. The branch E corresponds to the frequency mixing due to the quantum oscillation of the Fermi energy (see Sec.5).

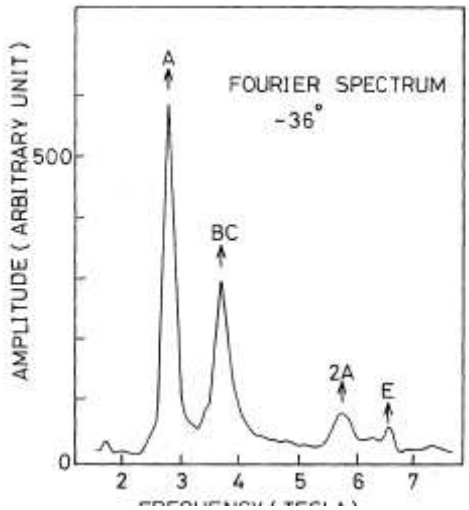

Fig.12 The Fourier spectrum of the dHvA oscillation. The magnetic field is oriented to make -36º from the *Z* axis in the *YZ* plane. The branches A, B, and C correspond to the *a*-, *b*-, and *c*-electron pockets, respectively.

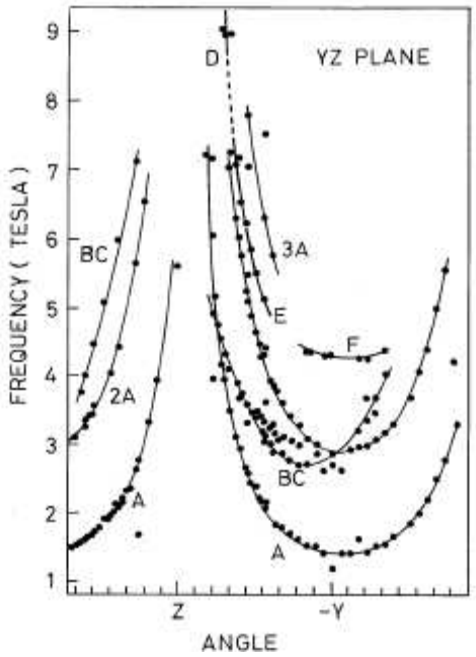

Fig.13 The angular dependence of the dHvA frequencies in the YZ plane. The branches A, *B*, and *C* correspond to the *a*-, *b*-, and *c*-electron pockets, respectively. The dHvA frequency F_F is approximately equal to F_{3A}, and F_D and F_E coincide with $F_A + F_{BC}$. Note that the *b*- and *c*- pockets separate into two branches in the range of the field angles from -48º to -70º, and this might be a result of the fact that the direction of magnetic field does not exactly lie in the *YZ* plane. Note that the frequency of α-oscillation is denoted as F_α where a means *A*, *BC*, *D*, *E*, 2*A* or 3*A*.

4.3 Result of dHvA effect in Bi (Bhargrava[7])

Table II The summary of results of dHvA effect in Bi.[7]

	Electrons			Holes	
	Periods in 10^{-5} G^{-1}		Area in 10^{12} cm^{-2} ellipsoidal	Periods in	Area in
Axes	Crystal axis	Ellipsoidal axis	axis	10^{-5} G^{-1}	10^{12} cm^{-2}
1	0.53±0.03	0.53 ±0.03	18.0	0.45 ±0.02	21.2
2	7.20±0.05 8.30±0.05	8.35 ±0.05	1.1	0.45 ±0.02	21.2
3	4.17±0.05 1.17±0.03	0.695±0.03	13.7	1.575±0.005	6.1

1: binary, 2: bisectrix, 3: trigonal

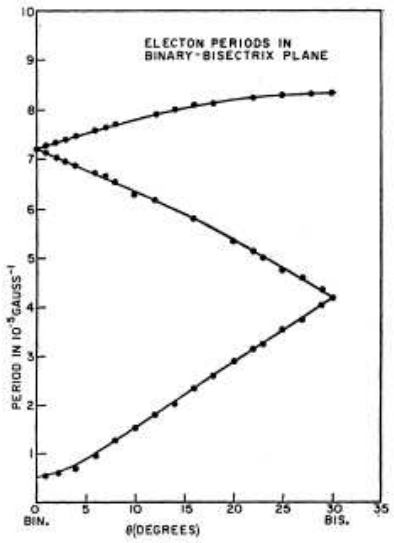

Fig.14 The angular dependence of electron dHvA period P in the XY plane for Bi. The solid line is a fit assuming an ellipsoidal Fermi surface and using the measured values of periods in the crystal axis and a tilt angle of 6.5º.[7]

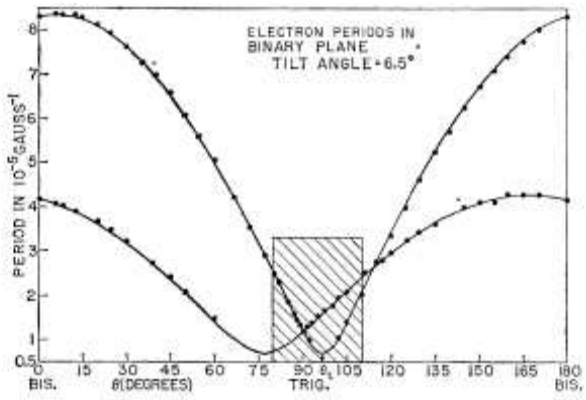

Fig.15 The angular dependence of electron dHvA periods in the YZ plane. The tilt angle measured is 6.50±0.25º. The shaded area shows the region where electron periods were never reported. The solid line is a fit using an ellipsoidal Fermi surface.[7]

5. Change of Fermi energy as a function of magnetic field

The dimension of the Fermi surface of Bi is very small compared with that of ordinary metals. Therefore the quantum number of the Landau level at the Fermi energy has a small value even at a low magnetic field. The Fermi energy varies with a magnetic field in a quasi oscillatory way, since the Landau level intervals of the hole and electrons are generally different to each other. The Fermi energy is determined from the charge neutrality condition that $N_h(B) = N_e^a(B) + N_e^b(B) + N_e^c(B)$. The field dependence of the Fermi energy in Bi is shown below when B is parallel to the binary, bisectrix, and trigonal axes, respectively.

We note that the dHvA frequency mixing has been observed in Bi by Suzuki et al.[10]. The Fermi energy changes at magnetic fields where the Landau level crosses the Fermi

energy, so that the Fermi energy shows a pseudo periodic variation with the field. This variation is remarkable even at low magnetic field in Bi. The observed frequency mixing is due to this effect.

(a) ***B*** // the binary axis (*X*)

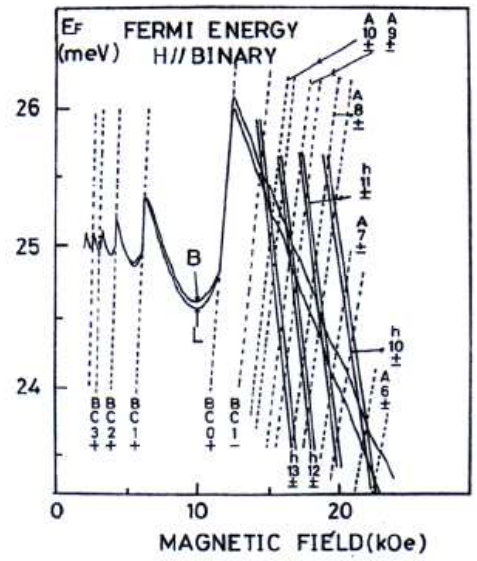

Fig.16 The magnetic field dependence of the Fermi energy (***B*** //*X*, T = 0 K). The dotted and solid lines correspond to the Landau levels of the electron and hole, respectively. The curve of E_F vs B exhibits kinks at the fields where the Landau levels cross the Fermi energy. *BCn*±: the Landau level of the electron *b*- and *c* pockets with the quantum number n and the spin up (+) (down (-)) -state. *hn*±: the Landau level of the hole pockets with the quantum number n and the spin up (+) (down (-)) -state. $E(n,\sigma) = \hbar\omega_c(n + \frac{1}{2} + \frac{1}{2}\nu_s\sigma)$, where ν_s is a spin-splitting factor defined in Sec.6.4, and $\sigma = \pm 1$. The expression of $E(n, \sigma)$will be discussed later. The ground Landau level is described by either Baraff[6] model (denoted B) or Lax[5] model (denoted by *L*).

(b) ***B*** // the bisectrix (*Y*)

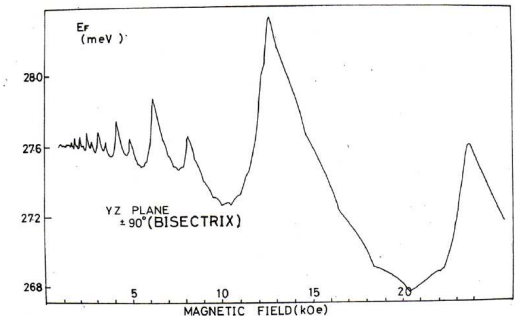

Fig.17 The magnetic field dependence of the Fermi energy (T = 0 K). Magnetic field is along the *Y* axis (bisectrix).[9,10]

(c) $\boldsymbol{B}$ //the trigonal axis (Z)

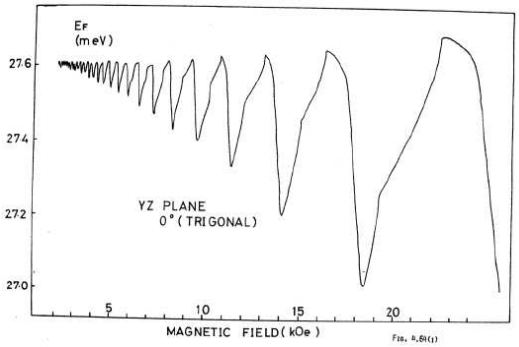

Fig.18 The magnetic field dependence of the Fermi energy (T = 0 K). Magnetic field is along the Z axis (trigonal).[9,10]

7. Motion of free electron in the presence of magnetic field

The energy of free electron is given by

$$E(\mathbf{k}) = \frac{\hbar^2}{2m}\mathbf{k}^2,$$

where m is the mass of electrons. The $\boldsymbol{k}$ space contours of constant energy are spheres and for a given $\boldsymbol{k}$ an electron has a group velocity given by

$$\mathbf{v}_\mathbf{k} = \frac{1}{\hbar}\nabla_\mathbf{k} E(\mathbf{k}). \tag{11}$$

The equation of motion of an electron in a magnetic field is given by

$$\hbar\frac{d\boldsymbol{k}}{dt} = -\frac{e}{c}\boldsymbol{v}\times\boldsymbol{B}. \tag{12}$$

This means that the change in the vector $\boldsymbol{k}$ is normal to the direction of $\boldsymbol{B}$ and is also normal to $\boldsymbol{v}$ (normal to the energy surface). Thus $\boldsymbol{k}$ must be confined to the orbit in the plane normal to $\boldsymbol{B}$. Since

$$\boldsymbol{v} = \boldsymbol{v}_k = (1/\hbar)\nabla_{\boldsymbol{k}}\varepsilon_{\boldsymbol{k}} = \frac{d\boldsymbol{r}}{dt}.$$

we have the equation of motion for electron as

$$\hbar\boldsymbol{k} = -\frac{e}{c}(\boldsymbol{r}-\boldsymbol{r}_0)\times\boldsymbol{B}, \tag{13}$$

where $\boldsymbol{r}_0$ [=(x_0, y_0)] is the position vector of the center of the orbit (guiding center). For simplicity we assume that $\boldsymbol{r}_0 = 0$.

$$\boldsymbol{k} = -\frac{e}{c\hbar}\boldsymbol{r} \times \boldsymbol{B}\,.$$

Suppose that the magnetic field is directed along the z axis. The position vector $\boldsymbol{r}$ and the wavevector $\boldsymbol{k}$ are in the same plane normal to the direction of the magnetic field $\boldsymbol{B}$.

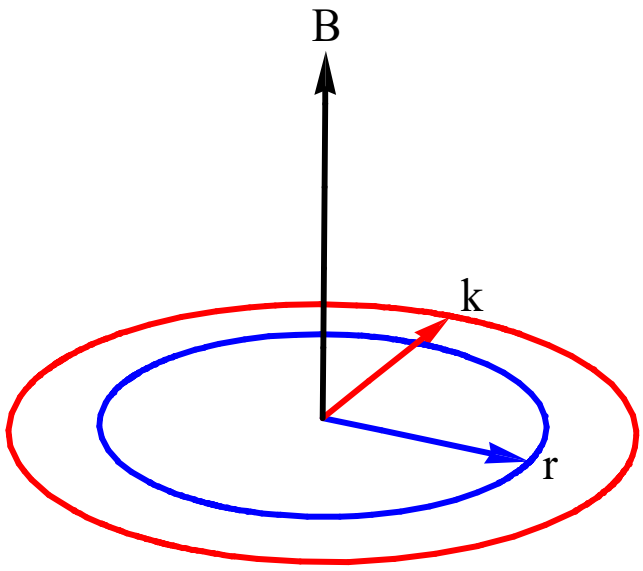

Fig.19 The position vector r and the wavevector $\boldsymbol{k}$ of free electron, in the 2D plane normal to the direction of the magnetic field $\boldsymbol{B}$ (along the z axis). $k = \frac{eB}{c\hbar}r = \frac{1}{\ell^2}r$. l is the magnetic length.

8. Analysis

When a magnetic field B is applied along the z axis, the electron motion in this direction is unaffected by this field, but in the (x, y) plane the Lorentz force induces a circular motion of the electrons. The Lorentz force causes a representative point in $\boldsymbol{k}$ space to rotate in the (k_x, k_y) plane with frequency

$$\omega_c = \frac{eB}{mc}$$

where -e is the charge of electron. This frequency, which is known as the cyclotron frequency, is independent of $\boldsymbol{k}$, so the whole system of the representative points rotate about an axis through the origin of $\boldsymbol{k}$ space and parallel to $\boldsymbol{B}$.

Analytically we get

$$x = \frac{c\hbar}{eB} k_y \,, y = -\frac{c\hbar}{eB} k_x \,, \tag{14}$$

In the complex plane, we have the relation,

$$x + iy = \frac{c\hbar}{eB} e^{-i\pi/2} (k_x + ik_y) = l^2 e^{-i\pi/2} (k_x + ik_y) \,. \tag{15}$$

This means that the magnitude of the position vector $\boldsymbol{r}$ of the electron is related to that of the wave vector $\boldsymbol{k}$ =(k_x, k_y) by a scaling factor

$$\eta = l^2 = \frac{c\hbar}{eB} \,.$$

The phase of the position vector is different from that of the wave vector by $-\pi/2$. l is so-called magnetic length.

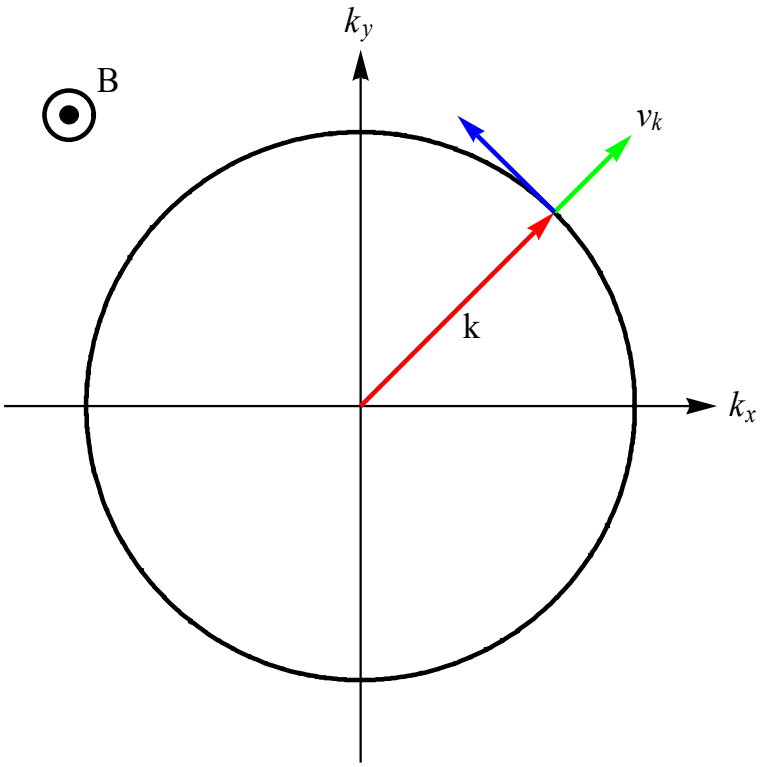

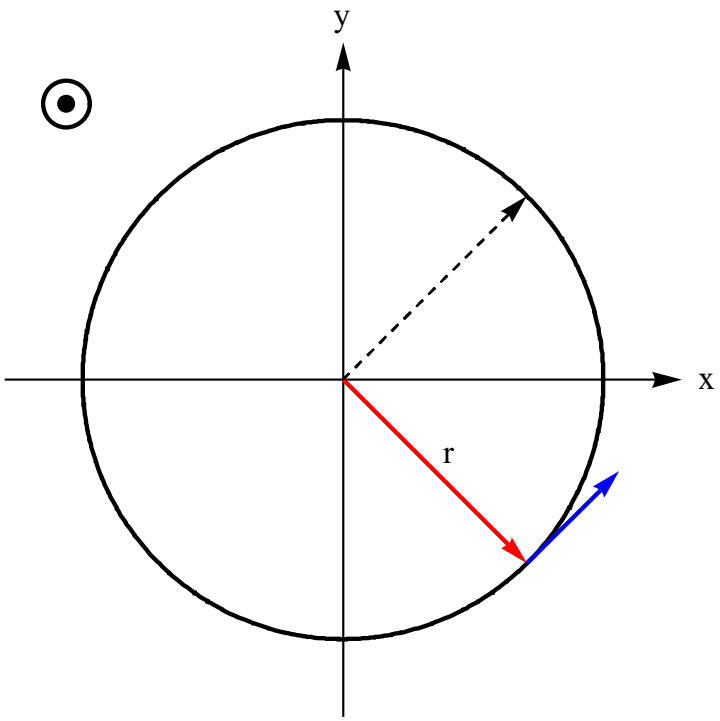

Fig.20 The orbital motion of electron in the presence of $\boldsymbol{B}$ ($\boldsymbol{B}$ is directed out of page) in the $\boldsymbol{k}$-space is similar to that in the $\boldsymbol{r}$-space but scaled by the factor η and through $\pi/2$.[12] Note that the directions of the x axis and y axis are the same as those of k_x axis and k_y axis, respectively.

9. Onsager theory: Semiclassical quantization of orbits in a magnetic field:

The Onsager-Lifshitz idea[2,11] was based on a simple semi-classical treatment of how electrons move in a magnetic field, using the Bohr-Sommerfeld condition to quantized the motion. The Lagrangian of the electron in the presence of electric and magnetic field is given by

$$L = \frac{1}{2}m\boldsymbol{v}^2 - q(\phi - \frac{1}{c}\boldsymbol{v}\cdot\boldsymbol{A}), \tag{16}$$

where m and q are the mass and charge of the particle.
Canonical momentum:

$$\boldsymbol{p} = \frac{\partial L}{\partial \boldsymbol{v}} = m\boldsymbol{v} + \frac{q}{c}\boldsymbol{A}. \tag{17}$$

Mechanical momentum:

$$\boldsymbol{\pi} = m\boldsymbol{v} = \boldsymbol{p} - \frac{q}{c}\boldsymbol{A}. \tag{18}$$

The Hamiltonian:

$$H = \boldsymbol{p}\cdot\boldsymbol{v} - L = (m\boldsymbol{v} + \frac{q}{c}\boldsymbol{A})\cdot\boldsymbol{v} - L = \frac{1}{2}m\boldsymbol{v}^2 + q\phi = \frac{1}{2m}(\boldsymbol{p} - \frac{q}{c}\boldsymbol{A})^2 + q\phi . \qquad (19)$$

The Hamiltonian formalism uses $\boldsymbol{A}$ and ϕ, and not $\boldsymbol{E}$ and $\boldsymbol{B}$, directly. The result is that the description of the particle depends on the gauge chosen.

We assume that the orbits in a magnetic field are quantized by the Bohr-Sommerfeld relation

$$\boldsymbol{\pi} = m\boldsymbol{v} = \hbar\boldsymbol{k} = \boldsymbol{p} - \frac{q}{c}\boldsymbol{A} = \boldsymbol{p} + \frac{e}{c}\boldsymbol{A} . \qquad (20)$$

and

$$\oint \boldsymbol{p}\cdot d\boldsymbol{l} = (n+\gamma)2\pi\hbar . \qquad (21)$$

where $q = -e$ ($e>0$) is the charge of electron, n is an integer, and γ is the phase correction: $\gamma = 1/2$ for free electron.

$$\oint \boldsymbol{p}\cdot d\boldsymbol{l} = \oint \hbar\boldsymbol{k}\cdot d\boldsymbol{l} - \frac{e}{c}\oint \boldsymbol{A}\cdot d\boldsymbol{l} = (n+\gamma)2\pi\hbar . \qquad (22)$$

Note we assume $\boldsymbol{r}_0 = 0$. Then we get

$$\oint \hbar\boldsymbol{k}\cdot d\boldsymbol{l} = -\frac{e}{c}\oint \boldsymbol{r}\times\boldsymbol{B}\cdot d\boldsymbol{l} = \frac{e}{c}\boldsymbol{B}\cdot\oint(\boldsymbol{r}\times d\boldsymbol{l}) = \frac{e}{c}\boldsymbol{B}\cdot 2A\boldsymbol{n} = \frac{2e}{c}\Phi . \qquad (27)$$

where

$$\oint(\boldsymbol{r}\times d\boldsymbol{l}) = 2 \text{ (area enclosed within the orbit) } \boldsymbol{n} \qquad \text{(geometrical result)}$$

and Φ is the magnetic flux contained within the orbit in real space, $\Phi = \boldsymbol{B}\cdot A\boldsymbol{n}$.

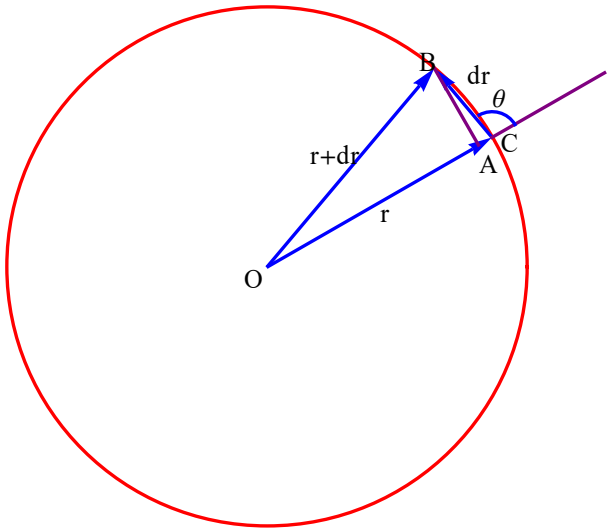

Fig.21 In this figure, we mean that $d\boldsymbol{r} = d\boldsymbol{l}$. The area of triangle OAB is equal to $|\boldsymbol{r} \times d\boldsymbol{l}|/2$.

$$\boldsymbol{r} \times d\boldsymbol{l} = \boldsymbol{n} r dr \sin\theta = \boldsymbol{n}\, \overline{OC} \cdot \overline{AB} = [2 \text{ area of } \Delta OAB\,]\ \boldsymbol{n}$$

where

$$\text{OC} = r, \qquad \text{AB} = dr \sin(\pi - \theta) = dr \sin\theta$$

Then we have

$$\oint (\boldsymbol{r} \times d\boldsymbol{l}) = 2 \text{ (area enclosed within the orbit) } \boldsymbol{n}$$

On the other hand,

$$-\frac{e}{c}\oint \boldsymbol{A} \cdot d\boldsymbol{l} = -\frac{e}{c}\oint (\nabla \times \boldsymbol{A}) \cdot d\boldsymbol{a} = -\frac{e}{c}\oint \boldsymbol{B} \cdot d\boldsymbol{a} = -\frac{e}{c}\Phi, \tag{28}$$

by the Stokes theorem. Then we have

$$\oint \boldsymbol{p} \cdot d\boldsymbol{l} = \frac{2e}{c}\Phi - \frac{e}{c}\Phi = \frac{e}{c}\Phi = (n+\gamma) 2\pi\hbar\,. \tag{29}$$

It follows that the orbit of an electron is quantized in such a way that the flux through it is

$$\Phi_n(\boldsymbol{r}) = (n+\gamma)\frac{2\pi\hbar c}{e} = 2\Phi_0(n+\gamma) \text{ (Onsager relation)}, \tag{30}$$

where Φ_0 is a quantum fluxoid and is given by

$$\Phi_0 = \frac{2\pi\hbar c}{2e} = \frac{hc}{2e} = 2.0678 \times 10^{-7} \text{ Gauss cm}^2. \quad (31)$$

Note that -2*e* corresponds to the charge of the Cooper pair (it will be discussed in the superconductivity).

((**Note**))

From p.217 (The development of the band theory of solids.
L. Hoddeson et al, Out of Crystal maze (Oxford University Press, 1992).

As Shoenberg's former research student Brian Pippard recalls, Shoenberg and Onsager shared an office during the latter's visiting year at Cambridge. But even after Onsager had written his paper, at least for a year or two, Cambridge physicists tended to give it little importance. Pippard recalls:

There was not a lovely lot of algebraic quantities and integrals which you could evaluate [in this paper] because Onsager was talking in geometrical terms - and I think David [Shoenberg] was disappointed to see "so little" coming out and failed to realize that Onsager had provided the complete clue. So nothing happened. The paper was published and nobody in Cambridge took any notice. They went on measuring the de Haas-van Alphen effect and fitting it with ellipsoidal shapes [in which the relation between energy and wave vector is assumed to be quadratic.

That was the situation at the end of 1952.

9. Physical meaning for the quantization of the magnetic flux

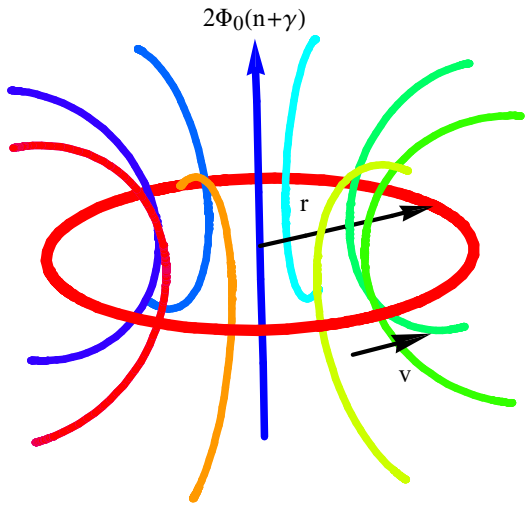

Fig.22 Quantization of the magnetic flux inside the orbit of electron (the real space). The number of the magnetic flux inside the orbit is only an integer.

According to the Onsager theory, the magnetic flux inside the orbit of electron is quantized as

$$\Phi_n(\boldsymbol{r}) = BS_n(\boldsymbol{r}) = (n+\gamma)\frac{2\pi\hbar c}{e} = 2\Phi_0(n+\gamma)$$

where $S_n(\boldsymbol{r})$ is the area of the electron orbit, and n is an integer. Using the relation

$$k = \frac{eB}{c\hbar}r = \frac{1}{\ell^2}r,$$

it is found that the area $S_n(\boldsymbol{k})$ of the orbit of electron in the $\boldsymbol{k}$-space (normal to $\boldsymbol{B}$) is related to the area $S_n(\boldsymbol{r})$ through

$$S_n(\boldsymbol{k}) = \frac{1}{Bl^4}BS_n(\boldsymbol{r}) = \frac{e^2B}{c^2\hbar^2}\Phi_n(\boldsymbol{r}) = \frac{2\pi eB}{\hbar c}(n+\gamma).$$

implying that $S_n(\boldsymbol{k})$ is also quantized for the fixed magnetic field B.

10. Definition of the magnetic length *l*

When the magnetic field $\boldsymbol{B}$ is applied to the z axis (normal to the plane), what is the area A where the quantum flux $2\Phi_0$ penetrates?

$$2\Phi_0 = \frac{2\pi\hbar c}{2e} = BS(\boldsymbol{r})$$

Then we get

$$S(\boldsymbol{r}) = \frac{\pi\hbar c}{eB} = \pi l^2.$$

where

$$l^2 = \frac{c\hbar}{eB}.$$

In other words, l is the radius of the circle inside which the quantum fluxoid Φ_0 passes through.

11. Physical meaning of the Onsager relation

We consider the Landau tubes whose cross sections by plane perpendicular to the direction of the magnetic field has the same area for the n-th Landau tube,

$$S_n(\boldsymbol{k}) = \frac{2\pi eB}{\hbar c}(n + \frac{1}{2}).$$

and are bounded by the curves of constant energy ($\frac{\hbar^2}{2m}k_z^{\,2} = \frac{\hbar^2}{2m}k_{//}^{\,2}$) at the height k_z in the $\boldsymbol{k}$-space. The energy at k_z of the Landau tube is given by

$$\varepsilon(n, k_z) = (n + \frac{1}{2})\hbar\omega_c + \frac{\hbar^2}{2m}k_z^{\,2}.$$

where ω_c is the cyclotron angular frequency,

$$\omega_c = \frac{eB}{mc}.$$

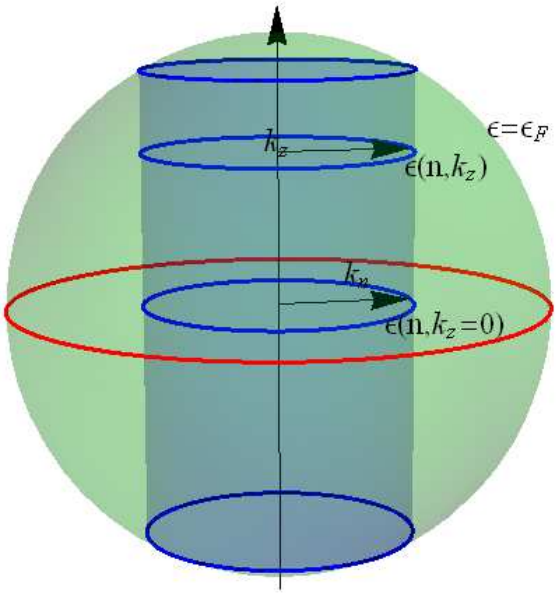

Fig.23 Landau tube in the ***k***-space. It is represented by the value of k_n (= $k_\perp$). The bottom and top parts of the Landau tube intersects with the Fermi surface. The magnetic field is directed along the z axis.

Here we show how to draw the Landau tubes:

(1) We choose the quantum number n (the integer) such

$$\frac{\hbar^2}{2m}k_\perp{}^2 = \hbar\omega_c(n+\frac{1}{2})$$

where $k_\perp$ (=k_n) n is the in-plane wavenumber.

(2) The energy of the cylinder (so-called Landau tube) at the point denoted by n and k_z is given by

$$\varepsilon(n,k_z) = \hbar\omega_c(n+\frac{1}{2}) + \frac{\hbar^2}{2m}k_z{}^2$$

The intersection of the constant-k_z plane with the Fermi surface (ε = ε_F) forms a cross section (circle with the radius k_n). The Landau tube can be constructed such that the top and the bottom are parts of the cylinder as shown in Fig.

The radius of the Landau tube denoted by the quantum number increases with increasing the magnetic field.

(a)

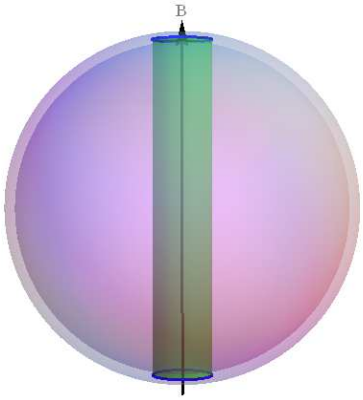

(b)

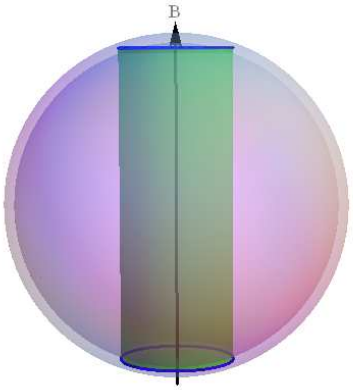

(c)

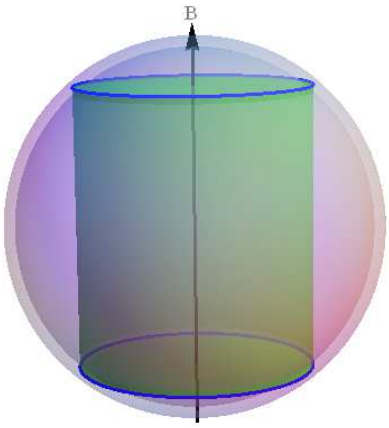

(d)

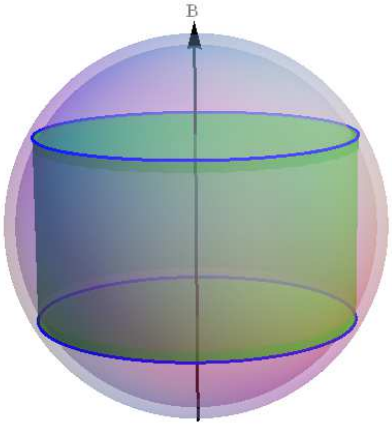

(e)

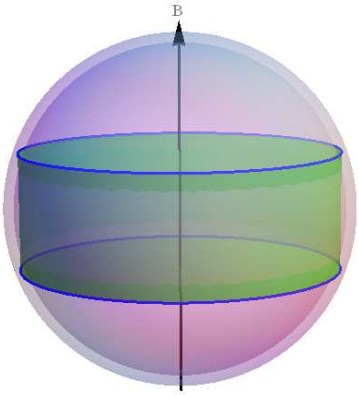

(f)

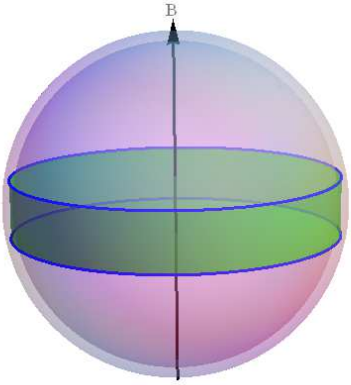

(g)

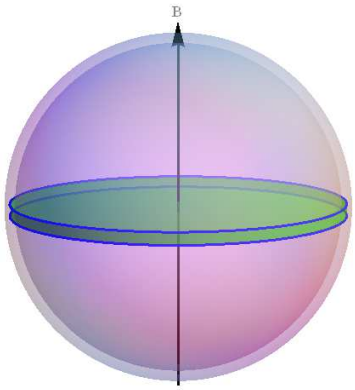

Fig.24 Landau tubes with the fixed n. The magnetic field is increased from (a) to (g)

The level density will have a sharp peak whenever ε is equal to the energy of an extremal orbit, satisfying the quantization condition. The reason for this is as follows. The above figures depict the Landau tube with the same n for different B. As the magnetic field B increases, the area of the Landau tube increases. The number of the states $D(\varepsilon)\mathrm{d}\varepsilon$ is proportional to the area of the portion of Landau tube contained between the constant-energy energy surfaces ε and $\varepsilon + \mathrm{d}\varepsilon$. The area of such a portion is not extremal in (a) to (f). The area of the portion as shown in (g) becomes extremal when there is an extremal orbit of energy ε on the Landau tube. Evidently, the area of the portion of the tube is enhanced as a result of the very slow energy variation of the level along the tube near the given orbit.

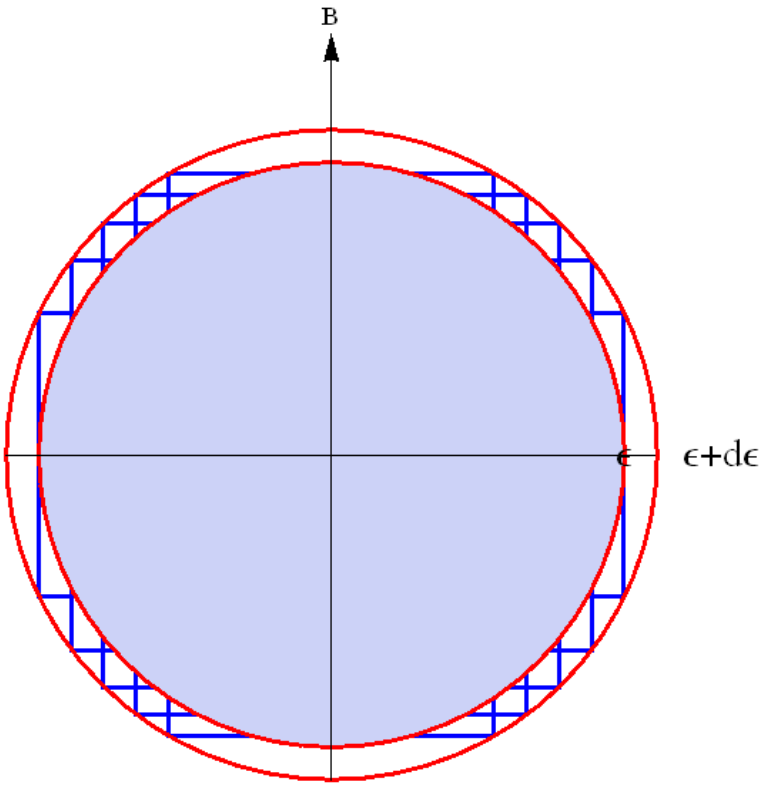

Fig.25 The number of the states $D(\varepsilon)\mathrm{d}\varepsilon$ which is proportional to the area of the portion of Landau tube contained between the constant energy surfaces ε and $\varepsilon + \mathrm{d}\varepsilon$. The region shaded by green.

12. Extremal orbit contributing to the dHvA signal

From the above discussion, we notice that the extremal value of the area of the cross-section of the Fermi surface, $A(\varepsilon_F, k_z)$, at the actual Fermi level ε_F, at the slice k_z, where k_z is the component of the wave vector along the direction of magnetic field $\boldsymbol{B}$. The extremal cross section is defined by

$$\frac{\partial A(\varepsilon_F, k_z)}{\partial k_z} = 0$$

at $k_z = k_0$.

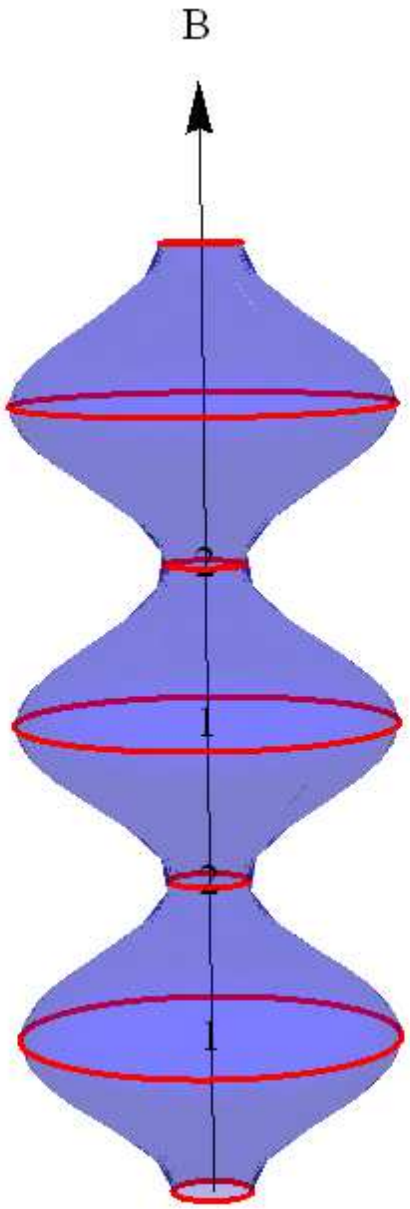

Fig.26 Extremal orbits 1 and 2. $A(\varepsilon_F, k_z)$ has a local maximum for the orbit 1 and has a local minimum for the orbit 2.

13. Landau tubes with the quantum number *n*

Here we draw a series of Landau tubes with different quantum number n for each fixed magnetic field *B*. We start with the relation given by

$$E = \frac{\hbar^2}{2m} k_z^{\,2} + \hbar\omega_c (n + \frac{1}{2})$$

where

$$\omega_c = \frac{eB}{mc}.$$

For simplicity, we assume that $\hbar = 1$, $m = 1$. Then we get

$$E = \frac{1}{2}k_z^{\,2} + \omega_c(n + \frac{1}{2})$$

For a fixed n (0 or positive integer) and a fixed E,

$$k_z = \pm\sqrt{2E - \omega_c(2n+1)}$$

The Landau tube consists of the cylinder with a radius

$$k_\perp = k_n = \sqrt{(2n+1)\omega_c}$$

and the length of cylinder

$$|k_z| \le \sqrt{2E - \omega_c(2n+1)}$$

We choose; $E = 12$. ω_c is changed as a parameter, where $\hbar = 1$ and $m = 1$.. In the quantum limit, there is only one state with n = 0 inside the Fermi surface. The Mathematica program is shown in the APPENDIX. We show the Landau tubes of quantized magnetic levels (n) at fixed values of $\hbar\omega_c$.

(a) $\hbar\omega_c$ = 0.5, 1, 1.5, and 2.0

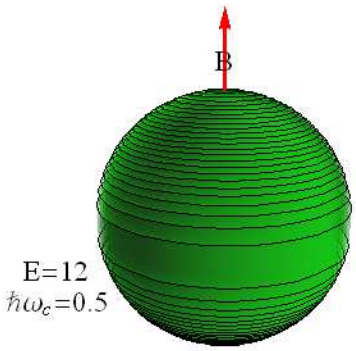

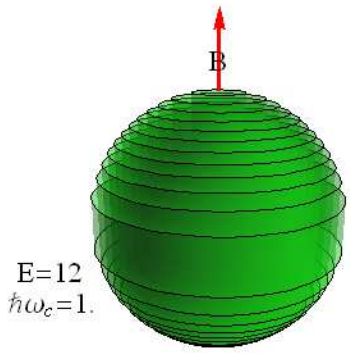

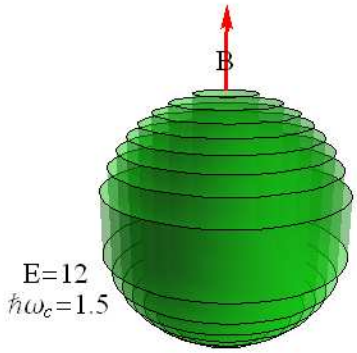

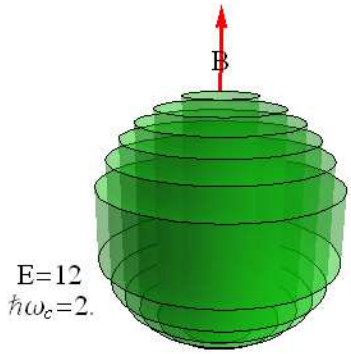

(b) $\hbar\omega_c$ = 2.5, 3, 3.5, and 4.0

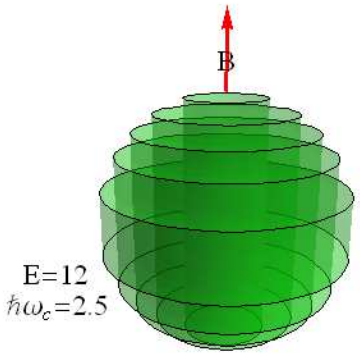

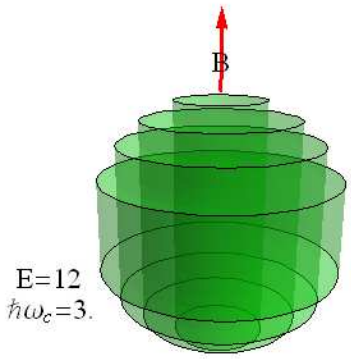

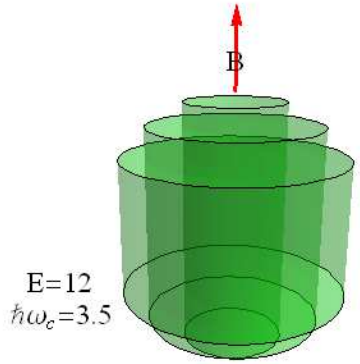

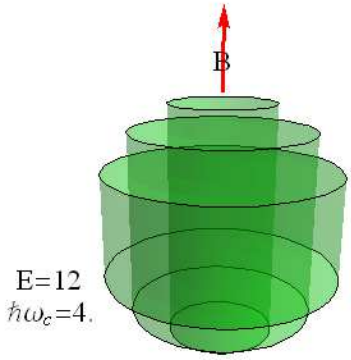

(c) $\hbar\omega_c$ = 4.5, 5, 5.5, and 6.0

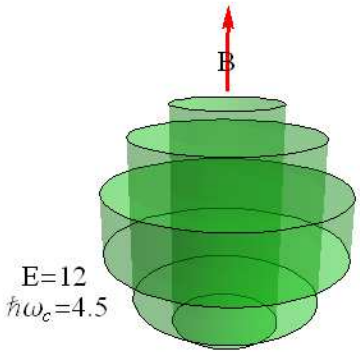

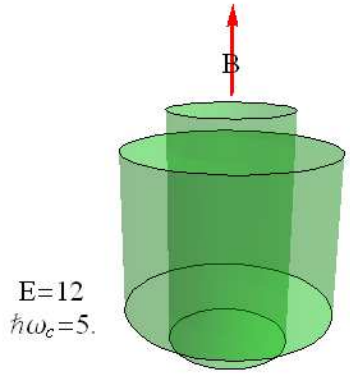

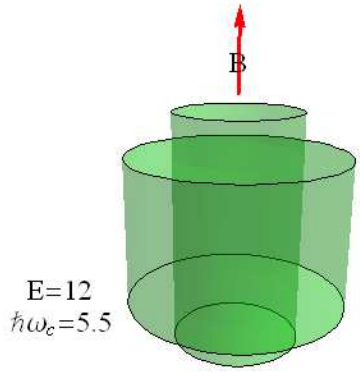

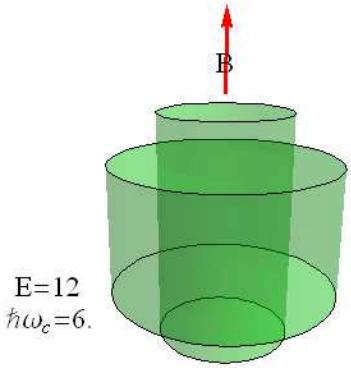

(d) $\hbar\omega_c$ = 6.5, 7, 7.5, 8.0

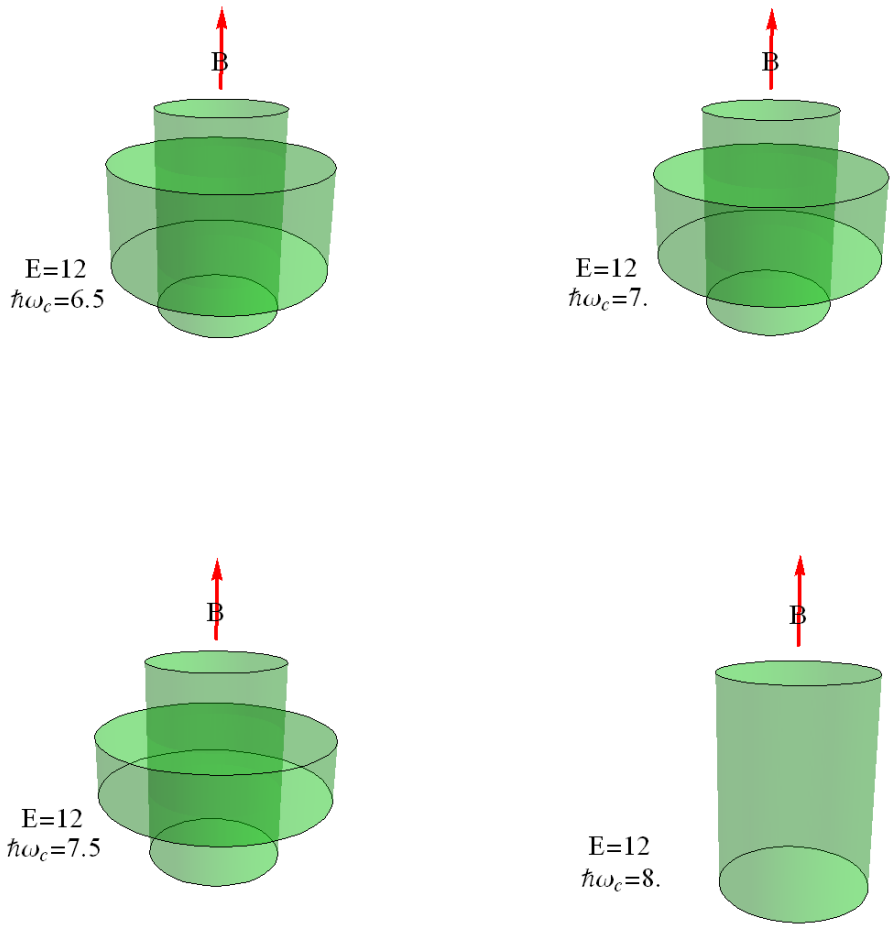

Fig.27

The last figure shows the quantum limit where only the Landau tube with n = 0 exists inside the Fermi surface.

14. Fundamentals of the Landau levels

We now consider the case when $k_z = 0$.

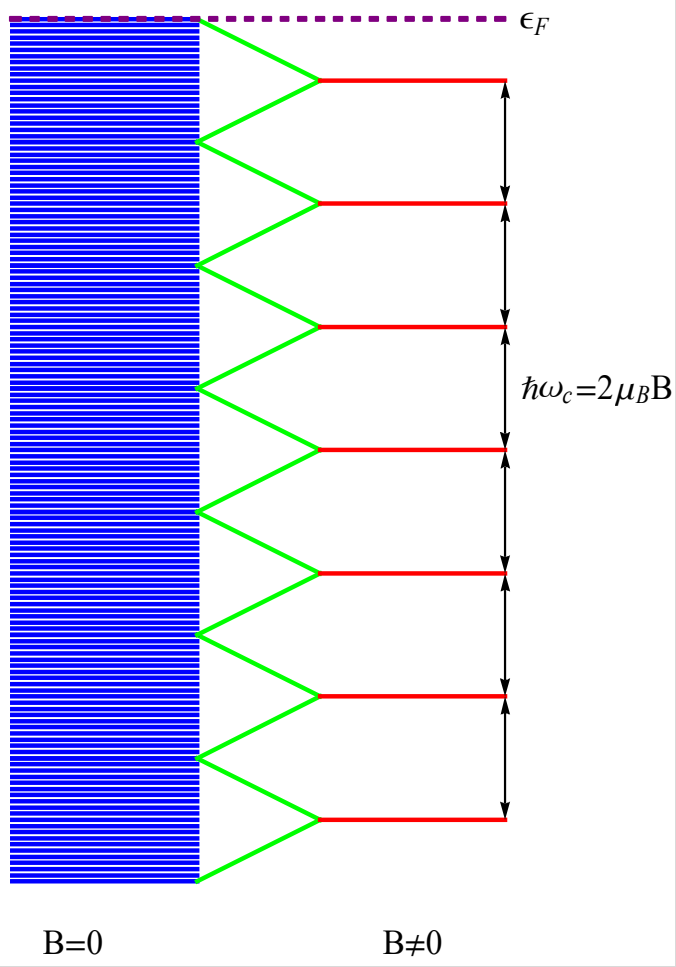

Fig.29

This regular periodic motion introduces a new quantization of the energy levels (Landau levels) in the (k_x, k_y) plane, corresponding to those of a harmonic oscillator with frequency ω_c and energy

$$\varepsilon_n = \hbar\omega_c(n+\frac{1}{2}) = \frac{\hbar^2}{2m}k_\perp{}^2, \qquad (12)$$

where $k_\perp$ is the magnitude of the in-plane wave vector and the quantum number n takes integer values 0, 1, 2, 3,..... ω_c is the cyclotron angular frequency and is defined by

$$\omega_c = \frac{eB}{mc}.$$

Each Landau ring is associated with an area of $\boldsymbol{k}$ space. The area S_n is the area of the orbit n with the radius $k_\perp = k_n$

$$S_n(\boldsymbol{k}) = \pi k_n^{\,2} = \frac{2\pi eB}{\hbar c}\left(n+\frac{1}{2}\right) = \frac{2\pi}{\ell^2}\left(n+\frac{1}{2}\right). \tag{13}$$

Thus in a magnetic field the area of the orbit in $\boldsymbol{k}$ space is quantized. Note that

$$l^2 = \frac{\hbar c}{eB}.$$

l is given by

$$l = \frac{256.556}{\sqrt{B[T]}}\ [\mu\mathrm{m}]$$

in the SI units.

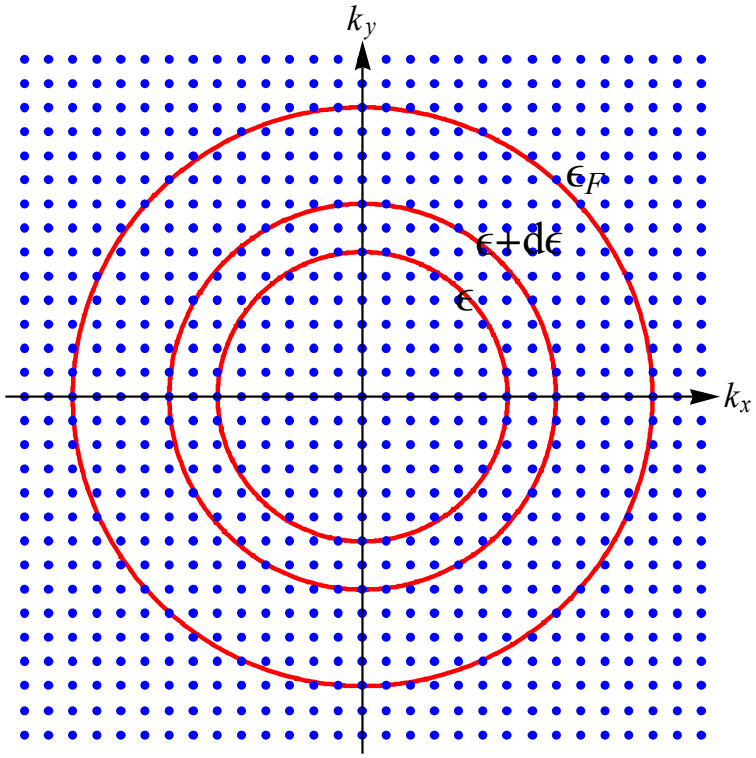

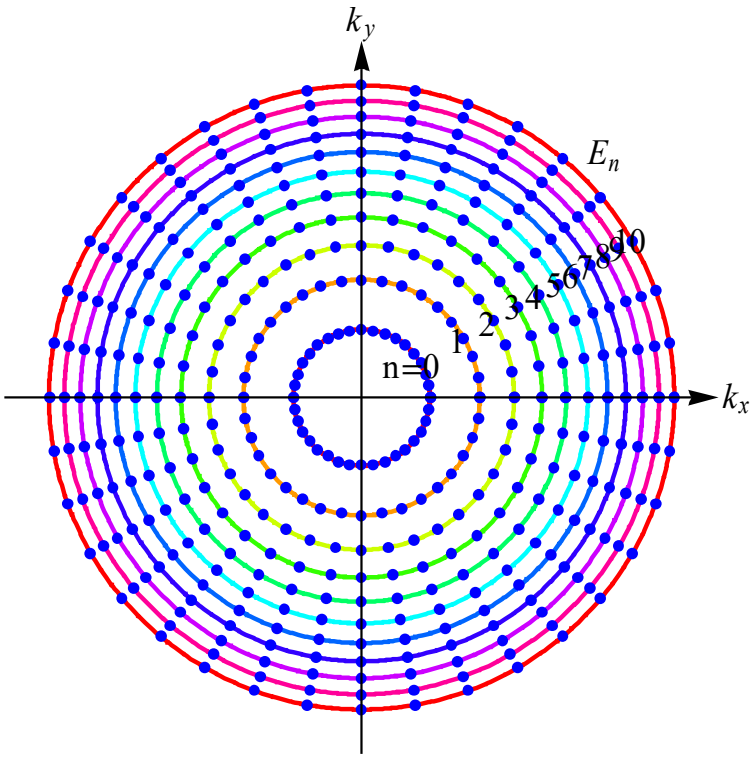

Fig.30 Quantization scheme for free electrons. Electron states are denoted by points in the $\boldsymbol{k}$ space in the absence and presence of external magnetic field $\boldsymbol{B}$. The states on each circle are degenerate. (a) When $\boldsymbol{B}$ = 0, there is one state per area $(2\pi/L)^2$. L^2 is the area of the system. (b) When $\boldsymbol{B} \neq 0$, the electron energy is quantized into Landau levels. Each circle represents a Landau level with energy $E_n = \hbar\omega_c(n+1/2)$.

15. Density of states using the magnetic length

We consider the density of states for the 2D system

$$D_o(\varepsilon)d\varepsilon = \frac{L^2}{(2\pi)^2} 2\pi k dk$$

where the electron spin is neglected. The energy dispersion relation is given by

$$\varepsilon_\perp = \frac{\hbar^2}{2m} k_\perp{}^2,$$

with

$$d\varepsilon_\perp = \frac{\hbar^2}{m} k_\perp dk_\perp$$

Then we get

$$D_o(\varepsilon_\varphi)d\varepsilon_\perp = \frac{L^2}{(2\pi)^2}2\pi\frac{m}{\hbar^2}d\varepsilon_\perp,$$

or

$$D_o(\varepsilon) = \frac{L^2}{(2\pi)^2}2\pi\frac{m}{\hbar^2} = \frac{mL^2}{2\pi\hbar^2}$$

which is constant. Note that we neglect the electron spin, since only the orbital motion is concerned.

Now we calculate the number of states between the adjacent energy levels ε_n and ε_{n+1}. Since

$$\Delta\varepsilon_\perp = \varepsilon_{n+1} - \varepsilon_n = \hbar\omega \quad \text{(which is independent of the quantum number } n\text{)}$$

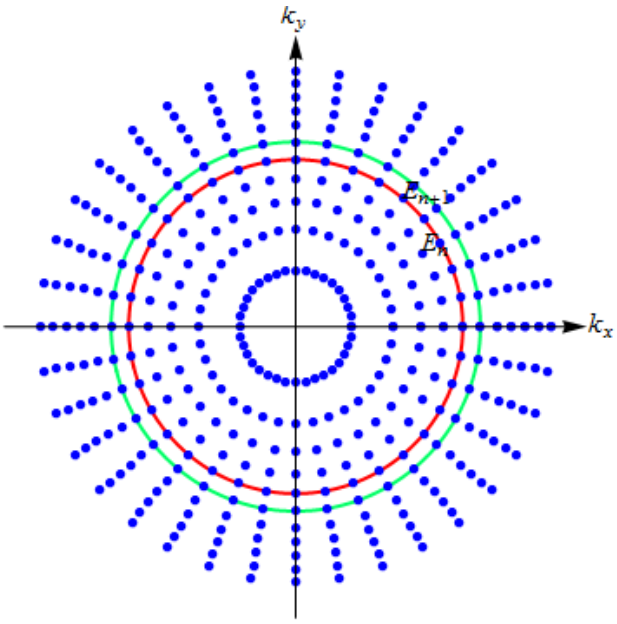

Fig.31 In a magnetic field the points in the (k_x, k_y) plane may be viewed as restricted circles

Then the number of states is calculated as

$$D = D(\varepsilon_\perp)\Delta\varepsilon_\perp = \frac{mL^2}{2\pi\hbar^2}\Delta\varepsilon_\perp = \frac{mL^2}{2\pi\hbar^2}\hbar\omega_c = \frac{mL^2}{2\pi\hbar^2}\frac{\hbar eB}{mc} = \frac{eBL^2}{2\pi\hbar c} = \rho B\,.$$

where

$$\rho = \frac{eL^2}{2\pi\hbar c}.$$

and

$$l^2 = \frac{c\hbar}{eB}.$$

16. Derivation of the dHvA frequency

(1) The use of the Onsager's relation

In the dHvA we need the area of the orbit in the $\boldsymbol{k}$-space. We define $S_n(\boldsymbol{r})$ as an area enclosed by the orbit in the real space ($\boldsymbol{r}$) and $S_n(\boldsymbol{k})$ as an are enclosed by the orbit in the $\boldsymbol{k}$-space. Then we have a relation

$$S_n(\boldsymbol{r}) = \left(\frac{c\hbar}{eB}\right)^2 S_n(\boldsymbol{k}) = l^4 S_n(\boldsymbol{k}). \tag{14}$$

and

$$S_n(\boldsymbol{k}) = (n+\gamma)\frac{2\pi e}{\hbar c}B. \tag{15}$$

In the Fermi surface experiments we may be interested in the increment ΔB for which two successive orbits, n and n+1, have the same area in the $\boldsymbol{k}$-space on the Fermi surface. Suppose that $S(\boldsymbol{k})$ is the Fermi surface in the momentum space. Then we have

$$S_n(\boldsymbol{k}) = S_{n+1}(\boldsymbol{k}) = S(\boldsymbol{k}),$$

or

$$(n+\gamma)\frac{2\pi e}{\hbar c}B_n = (n+1+\gamma)\frac{2\pi e}{\hbar c}B_{n+1} = S(\mathbf{k}),$$

or

$$\frac{S(\mathbf{k})}{B_n} = (n+\gamma)\frac{2\pi e}{\hbar c}, \qquad \frac{S(\mathbf{k})}{B_{n+1}} = (n+1+\gamma)\frac{2\pi e}{\hbar c}, \tag{16}$$

or

$$S(\mathbf{k})\left(\frac{1}{B_n} - \frac{1}{B_{n+1}}\right) = \frac{2\pi e}{\hbar c}. \tag{17}$$

or

$$\Delta(\frac{1}{B}) = \frac{2\pi e}{\hbar c S(\boldsymbol{k})} = \frac{1}{F}.$$

The dHVA frequency F is related to the area of the Fermi surface.

$$F = \frac{\hbar c}{2\pi e} S(\boldsymbol{k})$$

What is a typical value of ΔB which is experimentally observed?

$$\left|\Delta(\frac{1}{B})\right| = \frac{|\Delta B|}{B^2} = \frac{2\pi e}{\hbar c S(\boldsymbol{k})}. \qquad (18)$$

For Au,

$S(\boldsymbol{k})$=4.8 x 10^{16} cm^{-2} for the belly orbit of Au.

$$|\Delta B| = \frac{2\pi e}{\hbar c S(\boldsymbol{k})} B^2 = 0.198872[B_0(T)]^2 \qquad \text{(in units of G)}$$

where B_0 is in the units of T. When B = 5 T (which means B_0 = 5), we have

$$|\Delta B| = 4.97 \text{ G (= Oe).}$$

(2) The use of Landau level

Suppose that n-th Landau level exists just below the Fermi energy. The total number of states below the Fermi energy is

$$n\rho B = \frac{L^2}{(2\pi)^2} S(\boldsymbol{k}),$$

where $S(\boldsymbol{k})$ is the 2D extremal cross section of the Fermi surface, normal to $\boldsymbol{B}$, and ρ is

$$\rho = \frac{eL^2}{2\pi c\hbar}$$

Then we get

$$n\frac{e}{c\hbar} B = \frac{1}{2\pi} S(\boldsymbol{k})$$

or

$$\frac{1}{B_n} = n\frac{2\pi e}{\hbar c S(\boldsymbol{k})}$$

Similarly we get

$$\frac{1}{B_{n+1}} = (n+1)\frac{2\pi e}{\hbar c S(\boldsymbol{k})}$$

Then we have

$$\Delta(\frac{1}{B}) = \frac{1}{B_{n+1}} - \frac{1}{B_n} = \frac{2\pi e}{\hbar c S(k)} = \frac{1}{F}$$

This result is the same as that derived from the Onsager relation.

17. Another method for the derivation: cyclotron frequency

Note that the formula for can also be derived from the correspondence principle. The frequency for motion along a closed orbit is

$$\omega_c = \frac{eB}{m_c c}, \tag{19}$$

where ω_c is defined as

$$m_c = \frac{\hbar^2}{2\pi}\frac{\partial S}{\partial \varepsilon}, \tag{20}$$

In the semiclassical limit, one should obtain equidistant levels with a separation $\Delta\varepsilon$ equal to $\hbar\omega_c$. Hence

$$\Delta\varepsilon = \hbar\omega_c = \frac{\hbar eB}{m_c c} = \frac{\hbar eB}{c\left(\frac{\hbar^2}{2\pi}\frac{\partial S}{\partial \varepsilon}\right)} = \frac{2\pi eB}{c\hbar(\partial S/\partial\varepsilon)}, \tag{21}$$

or

$$\frac{\partial S}{\partial \varepsilon} = \frac{2\pi eB}{c\hbar}\frac{1}{\hbar\omega_c}. \tag{22}$$

or

$$\frac{\partial S_n(\boldsymbol{k})}{\partial \varepsilon} = \frac{2\pi eB}{c\hbar}\frac{1}{\hbar\omega_c}$$

or

$$S_n(\boldsymbol{k}) = \frac{2\pi eB}{c\hbar}\frac{1}{\hbar\omega_c}\hbar\omega_c(n+\gamma) = \frac{2\pi eB}{c\hbar}(n+\gamma)$$

18. Quantum mechanics

18.1 Landau gauge, symmetric gauge, and gauge transformation

$$H = \frac{1}{2m}(\mathbf{p} - \frac{q}{c}\mathbf{A})^2 + q\phi = \frac{1}{2m}(\mathbf{p} + \frac{e}{c}\mathbf{A})^2 - e\phi\,. \tag{23}$$

In the presence of the magnetic field ***B*** (constant), we can choose the vector potential as

$$\mathbf{A} = \frac{1}{2}(\mathbf{B}\times\mathbf{r}) = \frac{1}{2}\begin{vmatrix} \mathbf{e}_x & \mathbf{e}_y & \mathbf{e}_z \\ 0 & 0 & B \\ x & y & z \end{vmatrix} = \frac{1}{2}(-By, Bx, 0) \text{ (symmetric gauge).} \tag{24}$$

Here we define a gauge transformation between the vector potentials ***A*** and ***A***',

$$\mathbf{A}' = \mathbf{A} + \nabla\chi\,,$$

where $\chi = \frac{1}{2}Bxy$. Since

$$\nabla\chi = \frac{1}{2}B(y, x, 0)\,, \tag{25}$$

the new vector potential $\mathbf{A}'$ is obtained as

$$\mathbf{A}' = (0, Bx, 0) \qquad \text{(Landau gauge).} \tag{26}$$

The corresponding gauge transformation for the wave functions,

$$\psi'(\mathbf{r}) = \exp(\frac{iq\chi}{c\hbar})\psi(\mathbf{r}) = \exp(\frac{-ieB}{2c\hbar}xy)\psi(r)\,, \tag{27}$$

with q = -e (e>0).

18.2 Operators in quantum mechanics

We begin by the relation

$$\hat{\boldsymbol{\pi}} = \hat{\mathbf{p}} + \frac{e}{c}\mathbf{A}\,.$$

$$\begin{aligned}[\hat{\pi}_x, \hat{\pi}_y] &= [\hat{p}_x + \frac{e}{c}A_x, \hat{p}_y + \frac{e}{c}A_y] = \frac{e}{c}[\hat{p}_x, A_y] - \frac{e}{c}[\hat{p}_y, A_x] \\ &= \frac{e\hbar}{ic}\frac{\partial A_y}{\partial \hat{x}} - \frac{e\hbar}{ic}\frac{\partial A_x}{\partial \hat{y}} = \frac{e\hbar}{ic}B_z\end{aligned}\,, \tag{28}$$

or

$$[\hat{\pi}_x, \hat{\pi}_y] = \frac{e\hbar}{ic}B_z\,, \tag{29}$$

where

$$\frac{\partial A_y}{\partial \hat{x}} - \frac{\partial A_x}{\partial \hat{y}} = B_z\,.$$

Similarly we have

$$[\hat{\pi}_y, \hat{\pi}_z] = \frac{e\hbar}{ic}B_x\,, \qquad \text{and} \qquad [\hat{\pi}_z, \hat{\pi}_x] = \frac{e\hbar}{ic}B_y\,, \tag{30}$$

Since $\boldsymbol{A}$ commute with $\hat{\boldsymbol{r}}$ ($\boldsymbol{A}$ is a function of $\hat{\boldsymbol{r}}$),

$$\begin{aligned}&[\hat{x}, \hat{\pi}_x] = [\hat{x}, \hat{p}_x] = i\hbar\,, \quad [\hat{y}, \hat{\pi}_y] = [\hat{y}, \hat{p}_y] = i\hbar\,, \qquad [\hat{z}, \hat{\pi}_z] = [\hat{z}, \hat{p}_z] = i\hbar\,. \\ &[\hat{x}, \hat{\pi}_y] = [\hat{x}, \hat{p}_y + \frac{e}{c}A_y] = 0\,, \quad [\hat{y}, \hat{\pi}_x] = [\hat{y}, \hat{p}_x + \frac{e}{c}A_x] = 0\,,\end{aligned} \tag{31}$$

When $\boldsymbol{B}$ = (0,0,B) or $B_z = B$,

$$[\hat{\pi}_x, \hat{\pi}_y] = \frac{e\hbar B}{ic}\,, \qquad [\hat{\pi}_y, \hat{\pi}_z] = 0\,, \qquad [\hat{\pi}_z, \hat{\pi}_x] = 0\,, \tag{32}$$

Note that

$$[\hat{\pi}_x, \hat{\pi}_y] = \frac{e\hbar^2 B}{ic\hbar} = -i\frac{\hbar^2}{\ell^2}\,, \tag{33}$$

where l is called as a magnetic length and it is a cyclotron radius for the ground state Landau level: $\ell^2 = c\hbar / eB$.

Here we define the operators $\hat{X}$ and $\hat{Y}$ for the guiding-center coordinates.

$$\hat{X} = \hat{x} - \frac{c}{eB}\hat{\pi}_y = \hat{x} - \frac{l^2}{\hbar}\hat{\pi}_y, \qquad \hat{Y} = \hat{y} + \frac{l^2}{\hbar}\hat{\pi}_x, \tag{34}$$

The commutation relation is given by

$$\begin{aligned}
&[\hat{X},\hat{Y}] = [\hat{x} - \frac{l^2}{\hbar}\hat{\pi}_y, \hat{y} + \frac{l^2}{\hbar}\hat{\pi}_x] = -\frac{l^2}{\hbar}[\hat{\pi}_x,\hat{x}] - \frac{l^2}{\hbar}[\hat{\pi}_y,\hat{y}] + \frac{l^4}{\hbar^2}[\hat{\pi}_x,\hat{\pi}_y] = il^2, \\
&[\hat{\pi}_x,\hat{X}] = [\hat{\pi}_x,\hat{x} - \frac{l^2}{\hbar}\hat{\pi}_y] = [\hat{\pi}_x,\hat{x}] - [\hat{\pi}_x,\frac{l^2}{\hbar}\hat{\pi}_y] = 0, \\
&[\hat{\pi}_x,\hat{Y}] = [\hat{\pi}_x,\hat{y} + \frac{l^2}{\hbar}\hat{\pi}_x] = [\hat{\pi}_x,\hat{y}] + [\hat{\pi}_x,\frac{l^2}{\hbar}\hat{\pi}_x] = 0.
\end{aligned} \tag{35}$$

When the uncertainties ΔX and ΔY are defined by $(\Delta X)^2 = <\hat{X}^2>$ and $(\Delta Y)^2 = <\hat{Y}^2>$, respectively, we have the uncertainty relation,

$$(\Delta X)^2(\Delta Y)^2 \geq (1/4)\left|\left\langle[\hat{X},\hat{Y}]\right\rangle\right|^2 = (1/4)l^4,$$

or

$$(\Delta X)(\Delta Y) \geq (1/2)l^2.$$

The Hamiltonian $\hat{H}$ is given by

$$\hat{H} = \frac{1}{2m}(\hat{\mathbf{p}} + \frac{e}{c}\mathbf{A})^2 = \frac{1}{2m}(\hat{\pi}_x^{\,2} + \hat{\pi}_y^{\,2}), \tag{36}$$

We define the creation and annihilation operators,

$$\hat{a} = \frac{\ell}{\sqrt{2}\hbar}(\hat{\pi}_x - i\hat{\pi}_y), \qquad \hat{a}^+ = \frac{\ell}{\sqrt{2}\hbar}(\hat{\pi}_x + i\hat{\pi}_y), \tag{37),(38}$$

or

$$\hat{\pi}_x = \frac{\hbar}{\sqrt{2}\ell}(\hat{a} + \hat{a}^+), \qquad \hat{\pi}_y = \frac{\hbar}{i\sqrt{2}\ell}(\hat{a}^+ - \hat{a}), \tag{39}$$

$$[\hat{a},\hat{a}^+]=\frac{\ell^2}{2\hbar^2}[\hat{\pi}_x-i\hat{\pi}_y,\hat{\pi}_x+i\hat{\pi}_y]=\frac{\ell^2}{\hbar^2}i[\hat{\pi}_x,\hat{\pi}_x]=\frac{\ell^2}{\hbar^2}i(-i\frac{\hbar^2}{\ell^2})=1,$$

$$\hat{\pi}_x{}^2+\hat{\pi}_y{}^2=\frac{\hbar^2}{2\ell^2}[(\hat{a}+\hat{a}^+)^2-(\hat{a}^+-\hat{a})^2]=\frac{\hbar^2}{\ell^2}(\hat{a}\hat{a}^++\hat{a}^+\hat{a})=\frac{\hbar^2}{\ell^2}(2\hat{a}^+\hat{a}+1),$$

Thus we have

$$\hat{H}=\frac{\hbar^2}{m\ell^2}(\hat{a}^+\hat{a}+\frac{1}{2})=\hbar\omega_c(\hat{a}^+\hat{a}+\frac{1}{2}), \tag{40}$$

where

$$\hbar\omega_c=\frac{\hbar^2}{m\ell^2}=\frac{\hbar^2}{m(c\hbar/eB)}=\frac{\hbar eB}{mc}.$$

When $\hat{a}^+\hat{a}=\hat{N}$, the Hamiltonian is described by

$$\hat{H}=\hbar\omega_c(\hat{N}+\frac{1}{2}). \tag{41}$$

We thus find the energy levels for the free electrons in a homogeneous magnetic field- also known as Landau levels.

18.3 Schrödinger equation (Landau gauge)

We consider the Hamiltonian given by

$$\hat{H}=\frac{1}{2m}[\hat{p}_x{}^2+(\hat{p}_y+\frac{e}{c}B\hat{x})^2+\hat{p}_z{}^2], \tag{42}$$

$$\hat{\pi}_x=\hat{p}_x, \qquad \hat{\pi}_y=\hat{p}_y+\frac{e}{c}B\hat{x}, \tag{43}$$

The guiding-center coordinates are

$$\hat{X}=\hat{x}-\frac{l^2}{\hbar}\hat{\pi}_y=\hat{x}-\frac{l^2}{\hbar}(\hat{p}_y+\frac{e}{c}B\hat{x})=-\frac{l^2}{\hbar}\hat{p}_y, \qquad \hat{Y}=\hat{y}+\frac{l^2}{\hbar}\hat{p}_x, \tag{44}$$

The Hamiltonian $\hat{H}$ commutes with $\hat{p}_y$ and $\hat{p}_z$

$$[\hat{H},\hat{p}_y]=0 \quad \text{and} \quad [\hat{H},\hat{p}_z]=0$$

The Hamiltonian $\hat{H}$ also commutes with $\hat{X}$: $[\hat{H},\hat{X}]=0$.

$$\hat{H}\left|n,k_y,k_z\right\rangle = E_n\left|n,k_y,k_z\right\rangle$$

and

$$\hat{p}_y\left|n,k_y,k_z\right\rangle = \hbar k_y\left|n,k_y,k_z\right\rangle, \text{ and } \hat{p}_z\left|n,k_y,k_z\right\rangle = \hbar k_z\left|n,k_y,k_z\right\rangle$$

$$\left\langle y\left|\hat{p}_y\right|n,k_y,k_z\right\rangle = \hbar k_y\left\langle y\left|n,k_y,k_z\right\rangle, \qquad \left\langle z\left|\hat{p}_y\right|n,k_y,k_z\right\rangle = \hbar k_y\left\langle y\left|n,k_y,k_z\right\rangle\right.\right.$$

or

$$\frac{\hbar}{i}\frac{\partial}{\partial y}\left\langle y\left|n,k_y,k_z\right\rangle = \hbar k_y\left\langle y\left|n,k_y,k_z\right\rangle, \quad \frac{\hbar}{i}\frac{\partial}{\partial z}\left\langle z\left|n,k_y,k_z\right\rangle = \hbar k_z\left\langle z\left|n,k_y,k_z\right\rangle\right.\right.\right.$$

Schrödinger equation

$$\frac{1}{2m}[(\frac{\hbar}{i}\frac{\partial}{\partial x})^2 + (\frac{\hbar}{i}\frac{\partial}{\partial y} + \frac{e}{c}Bx)^2 + (\frac{\hbar}{i}\frac{\partial}{\partial y})^2]\psi(x,y,z) = \varepsilon\psi(x,y,z), \tag{45}$$

$$\psi(x,y,z) = e^{ik_y y + ik_z z}\phi(x), \tag{46}$$

$$x = \frac{\xi}{\beta}, \quad \text{with} \quad \beta = \sqrt{\frac{m\omega_c}{\hbar}} = \sqrt{\frac{eB}{\hbar c}} = \frac{1}{\ell} \quad \text{and} \quad \omega_c = \frac{eB}{mc},$$

$$\xi_0 = \beta\frac{c\hbar k_y}{eB} = \sqrt{\frac{c\hbar}{eB}}k_y = \ell k_y.$$

We assume the periodic boundary condition along the *y* axis.

$$\psi(x,y+L_y,z) = \psi(x,y,z), \tag{47}$$

or

$$e^{ik_y L_y} = 1,$$

or

$$k_y = (2\pi/L_y)n_y \ \ (n_y\text{: integers}), \tag{48}$$

Then we have

$$\phi''(\xi) = [(\xi - \xi_0)^2 + \frac{c}{e\hbar B}(-2mE_1 + \hbar^2 k_z{}^2)]\phi(\xi)$$

We put

$$E_1 = \hbar\omega_c(n + \frac{1}{2}) + \frac{\hbar^2 k_z{}^2}{2m} \text{ (Landau level),} \tag{49}$$

or

$$2mE_1 = \hbar^2 k_z{}^2 + 2m\hbar\omega_c(n + \frac{1}{2}) = \hbar^2 k_z{}^2 + \frac{2eB\hbar}{c}(n + \frac{1}{2}),$$

$$\phi''(\xi) = [(\xi - \xi_0)^2 - (2n + 1)]\phi(\xi).$$

Finally we get a differential equation for $\phi(\xi)$.

$$\phi''(\xi) + [2n + 1 - (\xi - \xi_0)^2]\phi(\xi) = 0.$$

The solution of this differential equation is

$$\phi_n(\xi) = (\sqrt{\pi}2^n n!)^{-1/2} e^{-\frac{(\xi-\xi_0)^2}{2}} H_n(\xi - \xi_0), \tag{50}$$

with

$$\xi_0 = \sqrt{\frac{c\hbar}{eB}} k_y = \ell k_y,$$

$$\ell = \sqrt{\frac{c\hbar}{eB}},$$

$$x_0 = \frac{\xi_0}{\beta} = \ell\xi_0 = \ell^2 k_y$$

The coordinate x_0 is the center of orbits. Suppose that the size of the system along the x axis is L_x. The coordinate x_0 should satisfy the condition, $0<x_0<L_x$. Since the energy of the system is independent of x_0, this state is degenerate.

$$0 < x_0 = \frac{\xi_0}{\beta} = \ell\xi_0 = \ell^2 k_y < L_x, \tag{51}$$

or

$$\ell^2 k_y = \frac{2\pi}{L_y}\ell^2 n_y < L_x ,$$

or

$$n_y < \frac{L_x L_y}{2\pi\ell^2} .$$

Thus the degeneracy is given by the number of allowed k_y values for the system.

$$g = \frac{L_x L_y}{2\pi\ell^2} = \frac{A}{2\pi\ell^2} = \frac{A}{2\pi\frac{c\hbar}{eB}} = \frac{BA}{2\Phi_0} = \frac{\Phi}{2\Phi_0} , \qquad (52)$$

where

$$\Phi_0 = \frac{2\pi\hbar c}{2e} = 2.0678\times 10^{-7}$$ Gauss cm^2.

The energy dispersion is plotted as a function of k_z for each Landau level with the index n.

$$E(n,k_z) = \hbar\omega_c(n+\frac{1}{2}) + \frac{\hbar^2 {k_z}^2}{2m} . \qquad (53)$$

18.4 Physical meaning of the distance *l*

The wavefunction is given by

$$\phi_n(\xi) = (\sqrt{\pi}2^n n!)^{-1/2} e^{-\frac{(\xi-\xi_0)^2}{2}} H_n(\xi-\xi_0)$$

When $n = 0$ (the ground state),

$$\phi_{n=0}(\xi) = \langle \xi | 0 \rangle = \pi^{-1/4} e^{-\frac{\xi^2}{2}} H_{n=0}(\xi) = \pi^{-1/4} e^{-\frac{\xi^2}{2}}$$

where

$$H_{n=0}(\xi) = 1 .$$

Since

$$\xi = \frac{x}{l} ,$$

we have

$$|x\rangle = \frac{1}{\sqrt{l}}|\xi\rangle.$$

Using this relation, we have

$$\phi_{n=0}(x) = \langle x|0\rangle = \frac{1}{\sqrt{\sqrt{\pi}l}} e^{-\frac{x^2}{2l^2}}$$

or

$$|\phi_{n=0}(x)|^2 = \frac{1}{\sqrt{\pi}l} e^{-\frac{x^2}{l^2}}.$$

When $\sigma = \frac{l}{\sqrt{2}}$, this function can be rewritten as the normal distribution function,

$$|\phi_{n=0}(x)|^2 = \frac{1}{\sqrt{2\pi}\sigma} e^{-\frac{x^2}{2\sigma^2}},$$

where $\sigma = \frac{l}{\sqrt{2}}$ is the standard deviation. $\sigma^2 = \frac{l^2}{2}$ is the variance.

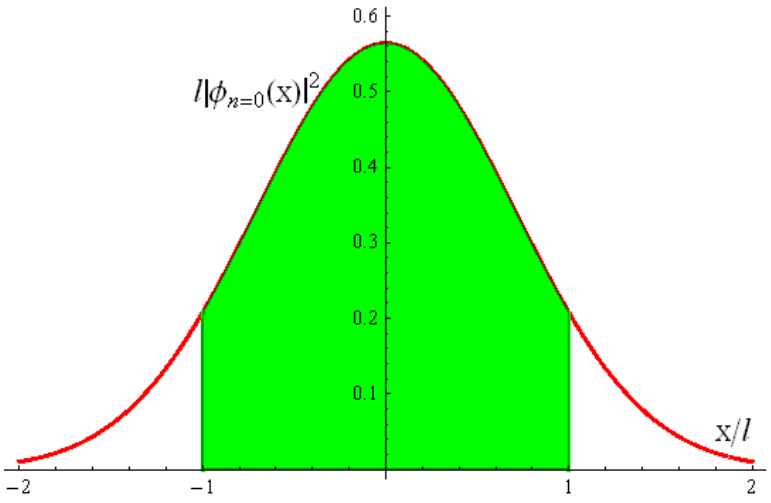

Fig.31 Plot of $l\left|\phi_{n=0}(x)\right|^2 = \frac{1}{\sqrt{\pi}} e^{-\frac{x^2}{l^2}}$ (ground state wave function) as a function of x/l, which is a Gaussian distribution function.

Here we note

$$\left\langle \xi' \middle| \xi'' \right\rangle = \delta(\xi' - \xi'') = \delta(\frac{x' - x''}{l}) = l\delta(x' - x'') = l\left\langle x' \middle| x'' \right\rangle$$

or

$$\left| x \right\rangle = \frac{1}{\sqrt{l}} \left| \xi \right\rangle .$$

19. Another method

$$\hat{H} = \frac{1}{2m}(\hat{\mathbf{p}} + \frac{e}{c}\mathbf{A})^2 = \frac{1}{2m}[\hat{\mathbf{p}}^2 + \frac{e^2}{c^2}\mathbf{A}^2 + \frac{e}{c}(\hat{\mathbf{p}} \cdot \mathbf{A} + \mathbf{A} \cdot \hat{\mathbf{p}})],$$

$$\begin{aligned} \hat{\mathbf{p}} \cdot \mathbf{A} + \mathbf{A} \cdot \hat{\mathbf{p}} &= \hat{p}_x A_x + \hat{p}_y A_y + \hat{p}_z A_z + A_x \hat{p}_x + A_y \hat{p}_y + A_z \hat{p}_z \\ &= [\hat{p}_x, A_x] + [\hat{p}_y, A_y] + [\hat{p}_z, A_z] + 2\mathbf{A} \cdot \hat{\mathbf{p}} \\ &= \frac{\hbar}{i} \nabla \cdot \mathbf{A} + 2\mathbf{A} \cdot \hat{\mathbf{p}} \end{aligned}$$

Then we have

$$\begin{aligned} \hat{H} &= \frac{1}{2m}[\hat{\mathbf{p}}^2 + \frac{e^2}{c^2}\mathbf{A}^2 + \frac{e}{c}(\frac{\hbar}{i}\nabla \cdot \mathbf{A} + 2\mathbf{A} \cdot \hat{\mathbf{p}})] \\ &= \frac{1}{2m}(\hat{\mathbf{p}}^2 + \frac{e^2}{c^2}\mathbf{A}^2 + \frac{e\hbar}{ic}\nabla \cdot \mathbf{A} + \frac{2e}{c}\mathbf{A} \cdot \hat{\mathbf{p}}) \end{aligned}$$

Since $\nabla \cdot \mathbf{A} = 0$,

$$\hat{H} = \frac{1}{2m}(\hat{\mathbf{p}}^2 + \frac{e^2}{c^2}\mathbf{A}^2 + \frac{2e}{c}\mathbf{A} \cdot \hat{\mathbf{p}}) = \frac{1}{2m}\hat{\mathbf{p}}^2 + \frac{e^2B^2}{2mc^2}\hat{x}^2 + \frac{eB}{mc}\hat{x}\hat{p}_y ,$$

where

$$\ell^2 = \frac{c\hbar}{eB}, \qquad \hbar\omega_c = \frac{\hbar^2}{m\ell^2} = \frac{\hbar eB}{mc}, \qquad m\omega_c{}^2 = \frac{e^2B^2}{mc^2},$$

$$\hat{H} = \frac{1}{2m}\hat{\mathbf{p}}^2 + \frac{e^2B^2}{2mc^2}\hat{x}^2 + \omega_c\hat{x}\hat{p}_y = \frac{1}{2m}\hat{\mathbf{p}}^2 + \frac{m\omega_c{}^2}{2}\hat{x}^2 + \omega_c\hat{x}\hat{p}_y .$$

The first and second terms of this Hamiltonian are that of the simple harmonics along the x axis.

This Hamiltonian $\hat{H}$ commutes with $\hat{p}_y$ and $\hat{p}_z$. Thus the wave function can be described by the form,

$$\psi(x,y,z) = \phi_n(x)e^{i(k_y y + k_z z)}.$$

20. The Zeeman splitting of the Landau level

Here we consider the effect of the spin magnetic moment on the Landau level.

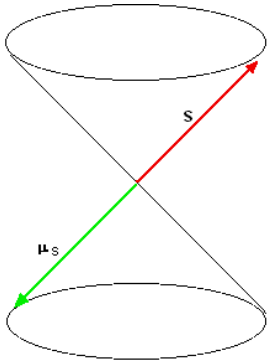

Fig.32 Spin angular momentum $\boldsymbol{S}$ and spin magnetic moment $\boldsymbol{\mu}_s$ for free electron. $\mathbf{S} = \hbar\boldsymbol{\sigma}/2$. $\boldsymbol{\mu}_s = -(2\mu_B \mathbf{S}/\hbar)$. $\mu_B = e\hbar/2m_0c$ (Bohr magnetron).

The spin magnetic moment $\boldsymbol{\mu}_s$ is given by $\boldsymbol{\mu}_s = -g\mu_B(\mathbf{S}/\hbar) = -(g\mu_B/2)\boldsymbol{\sigma}$, where $\mu_B = e\hbar/(2m_0c)$ (Bohr magneton). The factor g is called the Landé-g factor and is equal to g =2.0023 for free electrons. In the presence of magnetic field $\boldsymbol{B}$ along the z axis, the Zeeman energy is given by

$$-\boldsymbol{\mu}_s \cdot \mathbf{B} = \frac{g\mu_B}{2} B\sigma = \hbar\omega_c \frac{m_c}{m_0}\left(\frac{g\sigma}{2}\right) = \frac{1}{2}\hbar\omega_c \nu_s \sigma, \tag{54}$$

where $\nu_s = gm_c/m_0$ and $\sigma = \pm 1$. Thus we have the splitting of the Landau level in the presence of magnetic field as

$$E(n,\sigma) = \hbar\omega_c\left(n + \frac{1}{2} + \frac{1}{2}\nu_s\sigma\right). \tag{55}$$

where ν_s is much smaller than 1 for Bi.

21. Numerical calculations using Mathematica 5.2

21.1. Energy dispersion of the Landau level

We consider the energy dispersion of the Landau level with the quantum number n as a function of k_z.

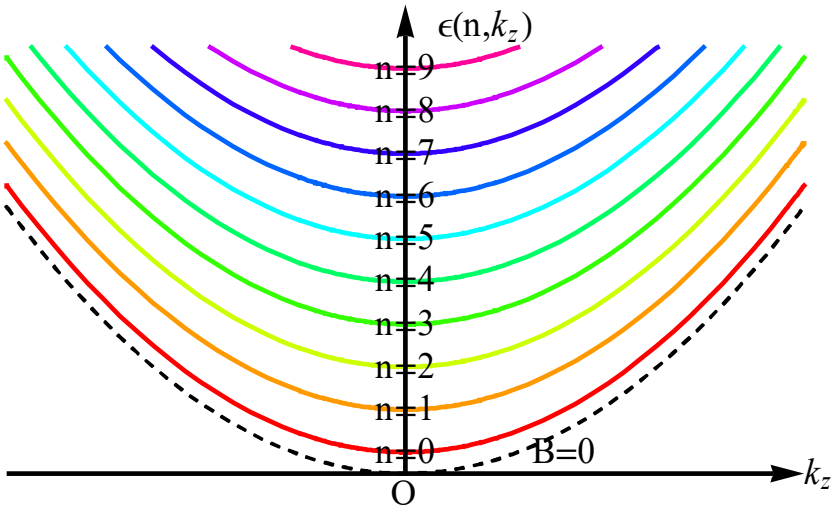

Fig.33 Energy dispersion of the Landau levels with n and k_z for a 3D electron gas in the presence of a magnetic field along the z axis.

21.2. Plot of the Landau wave function as a function of ξ, where $\xi_0 = 0$.

(a)

Plot of the wave function

$$\varphi_n(\xi) = (\sqrt{\pi}\, 2^n n!)^{-1/2} e^{-\xi^2/2} H_n(\xi)$$

where n = 0, 1, 2,...

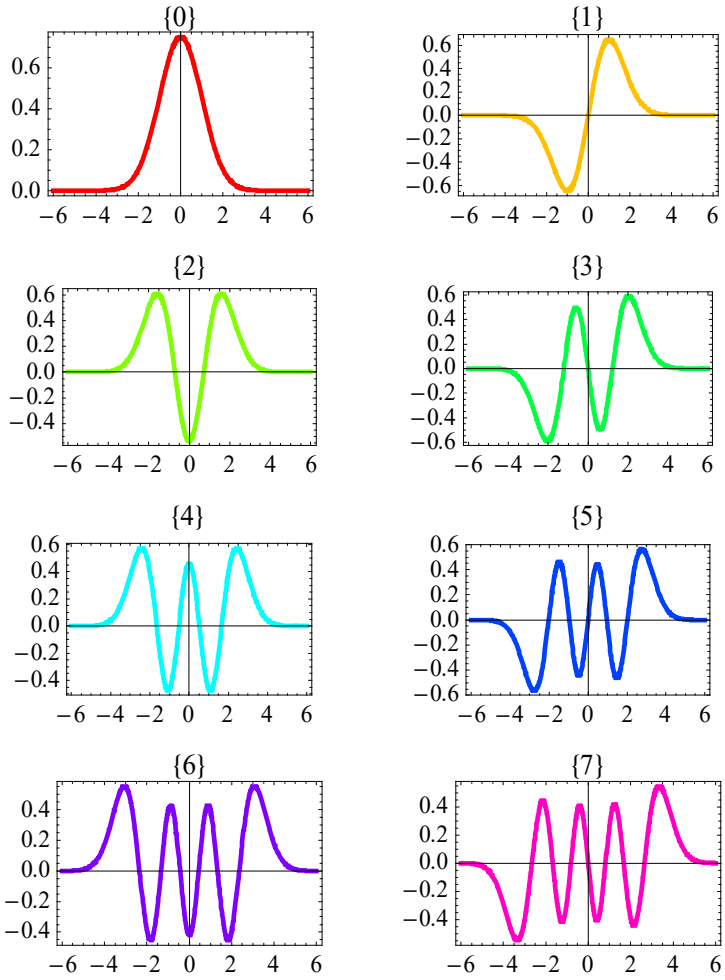

(b)

Plot of $\left|\varphi_n(\xi)\right|^2$ where $n = 0, 1, 2, \ldots,$

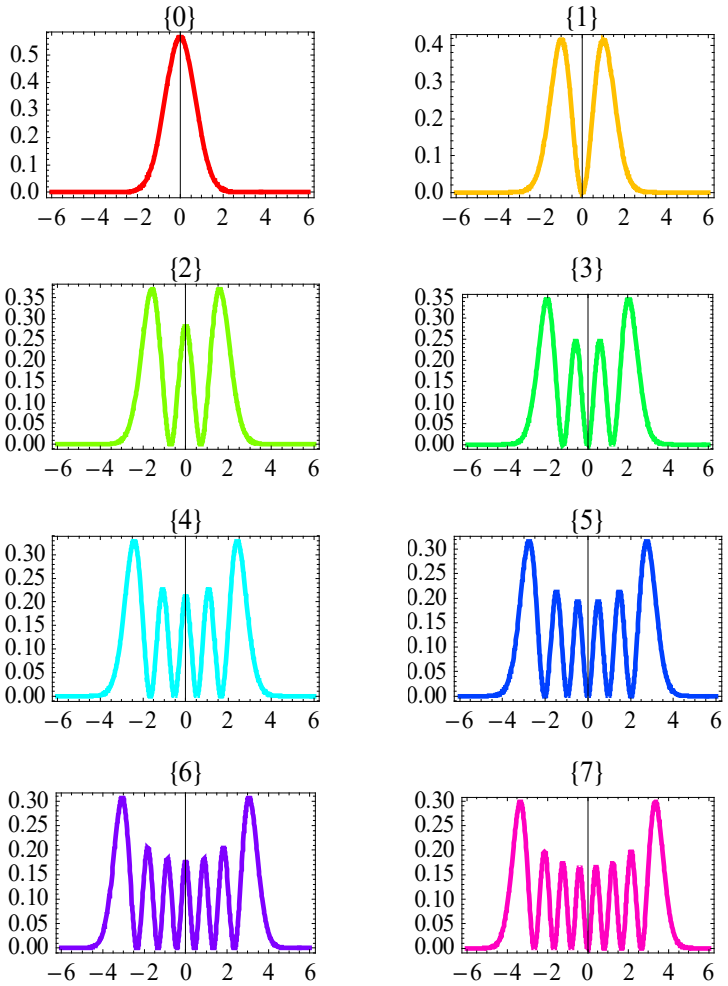

(b)

Fig.34 Plot of (a) $\phi_n(\xi)$ and (b) $|\phi_n(\xi)|^2$ with $\xi_0 = 0$ as a function of ξ. $n = 0$, 1, …,and 6.

21.3 Mathematica program

Landau level

```
Clear["Global`*"]; πx := ħ/i D[#, x] &; πy := (ħ/i D[#, y] + e B x/c #) &;
πz := ħ/i D[#, z] &;
f =
  1/(2 m) (Nest[πx, ψ[x, y, z], 2] + Nest[πy, ψ[x, y, z], 2] +
      Nest[πz, ψ[x, y, z], 2]) == E1 ψ[x, y, z] // Simplify;
rule1 = {ψ → (Exp[i ky #2 + i kz #3] ϕ[#1] &)};
rule2 = {β → Sqrt[e B/(ħ c)], ky → -Sqrt[e B/(c ħ)] ξ0, E1 → e B ħ/(m c) (n + 1/2) + ħ^2 kz^2/(2 m)};
vchange[Eq_, ψ_, x_, z_, f_] :=
  Eq /. {D[ψ[x], {x, n_}] :> Nest[(1/D[f, z] D[#, z] &), ψ[z], n],
    ψ[x] :> ψ[z], x :> f};
f1 = f /. rule1 // Simplify; seq1 = vchange[f1, ϕ, x, ξ, ξ/β] // FullSimplify;
seq2 = seq1 //. rule2 // FullSimplify;
rule3 = {ϕ → (h[#] Exp[-1/2 (# - ξ0)^2] &)};
seq3 = seq2 /. rule3 // FullSimplify
```

$$\frac{B e e^{i kz z-\frac{1}{2}(\xi-\xi0)^2-i y \xi0 \sqrt{\frac{B e}{c \hbar}}} \hbar (2 n h[\xi] + 2 (-\xi + \xi0) h'[\xi] + h''[\xi])}{m} == 0$$

```
DSolve[seq3, h[ξ], ξ] // Simplify[#, {n > 0, n ∈ Integers}] &
```

$$\{\{h[\xi] \to C[1]\ \text{HermiteH}[n, \xi - \xi0] + C[2]\ \text{Hypergeometric1F1}\left[-\frac{n}{2}, \frac{1}{2}, (\xi - \xi0)^2\right]\}\}$$

22. General form of the oscillatory magnetization (Lifshitz-Kosevich)

The expression of the oscillatory magnetization is derived by Lifshitz and Kosevich[11] as

$$M = -\frac{\sqrt{2}T(e\hbar/c)^{3/2}}{\pi^{3/2}B^{1/2}}\sum_e S_e\left|\frac{\partial^2 S}{\partial p_z^2}\right|_e^{-1/2}\exp(-\frac{2\pi^2 T c m_c}{e\hbar B})\sin(\frac{cS_e}{e\hbar B}\pm\frac{\pi}{4})\cos(\frac{\pi m_c}{m_0}), \quad (56)$$

where the sum over e extends all extremal cross-sectional are of the Fermi surface, the phase $+\pi/4$ if $\partial S/\partial p_z > 0$ (minimum) and $-\pi/4$ if $\partial S/\partial p_z < 0$ (maximum), m_0 is a mass of free electron, and $m_c = (1/2\pi)\partial S/\partial \varepsilon$. The term $\cos(\pi m_c/m_0)$ arises from the Zeeman splitting of spins. The magnetization oscillations are periodic in $1/B$. The period is

$$\Delta(\frac{1}{B}) = \frac{2\pi e\hbar}{cS_e}, \tag{57}$$

The influence of electron scattering is not taken into account in the derivation given above. Its effect is easily estimated. A proper account of the influence of collisions gives rise to an additional factor. If the mean time between collisions is τ, the corresponding uncertainty in electron energies $\hbar/\tau$ is equivalent to a temperature, so-called Dingle temperature

$$\exp(-\frac{2\pi^2 cm_c}{e\tau B}) = \exp(-\frac{2\pi^2 k_B T_d cm_c}{e\hbar B}), \tag{58}$$

where T_d is the Dingle temperature and is defined by

$$T_d = \frac{\hbar}{k_B \tau}.$$

23. Simple model to understand the dHvA effect[13,16]

Consider the figure showing Landau levels associated with successive values of $n = 0$, 1, 2, …, s The upper green line represents the Fermi level ε_F. The levels below ε_F are filled, those above are empty. Since ε_F is much larger than the level-separation $\hbar\omega_c$, the number $n = s$ of occupied levels is very large. Let us assume that the magnetic field is increased slightly. The level separation will increase, and one of the lower levels will eventually cross the Fermi level. The resulting distribution of levels is similar to the original one except that the number of filled levels below ε_F is now $n = s$-1, instead of $n = s$. Since n is large, this difference is essentially negligible, so that one expects the new state to be equivalent to the original one. This implies a periodic dependence of the magnetization.

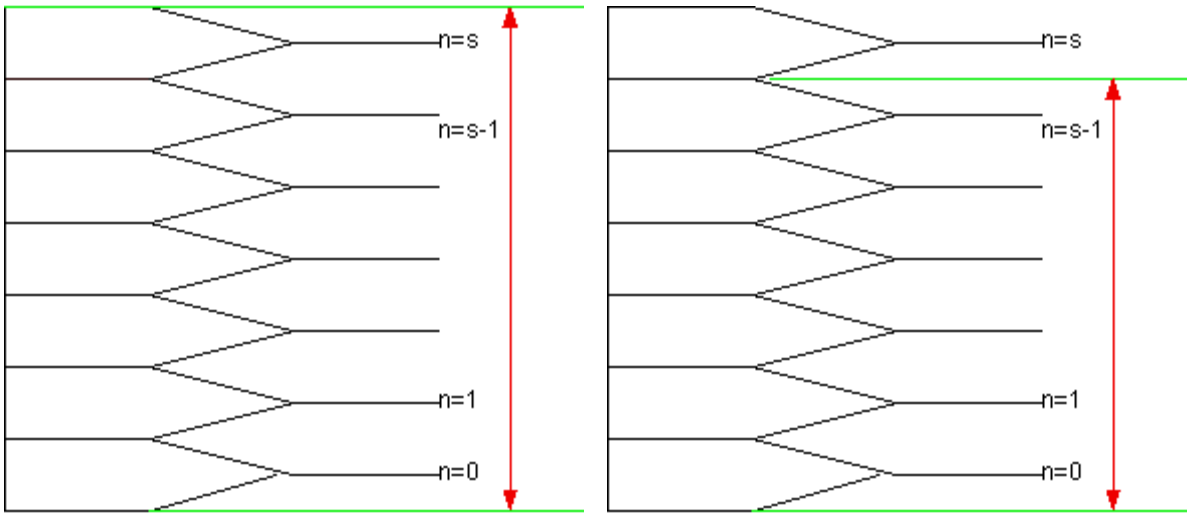

Fig.35 Schematic energy diagram of a 2D free electron gas in the absence and presence of B. At $B = 0$, the states below ε_F are occupied. The energy levels are split into the Landau levels with (a) $n = 0, 1, 2,\ldots$, and s for a specified field and (b) $n = 0, 1, 2,\ldots$, and s-1 for another specified field. The total energy of the electrons is the same as in the absence of a magnetic field.

((Mathematica)) Schematic energy diagram as a function of 1/B

This figure shows the schematic diagram of the location of each Landau levels as a function of $\varepsilon_F/\hbar\omega_c$. When $\varepsilon_F/\hbar\omega_c = s$ (integer), there are s Landau levels below the Fermi level ε_F.

```
Clear["Global`*"];
F1[x_, n_, i_] :=
 Which[x < n, 0, n ≤ x < n + 1, i/n, x > n + 1, 0];
Plot[
 Evaluate[Table[F1[x, n, i], {n, 1, 30}, {i, 1, n}]],
 {x, 0, 31},
 PlotStyle → Table[{Thickness[0.007], Hue[0.1 j]},
   {j, 0, 10}], PlotRange → {{0, 31}, {0, 1}}]
```

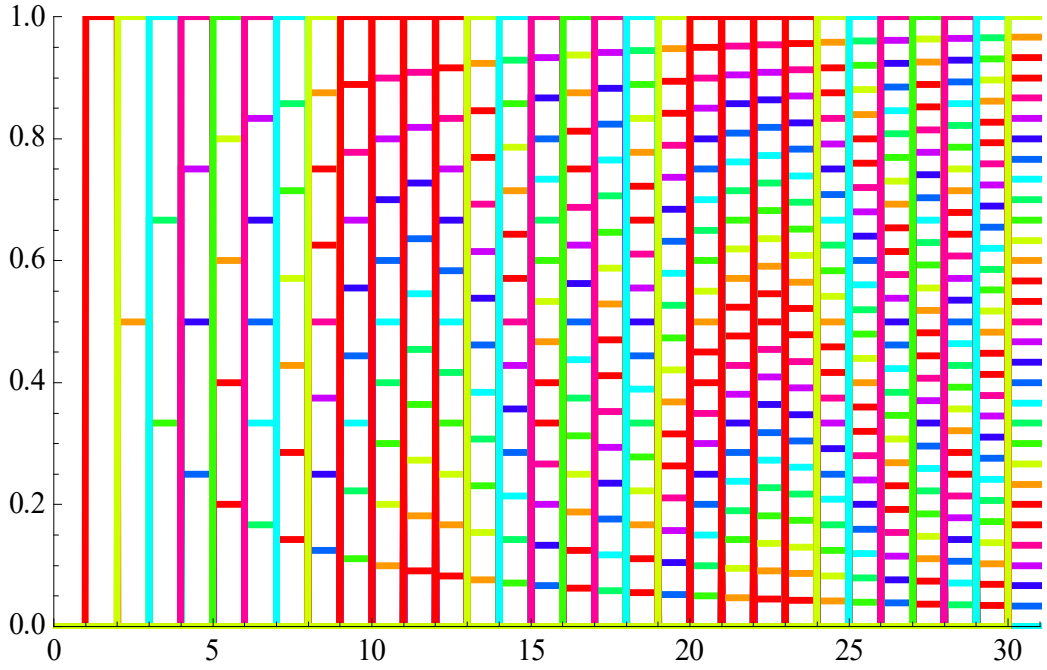

Fig.36 Schematic diagram for the separation of the Landau level as a function of $1/B$. The x axis is $s = N/(\rho B)$. The y axis is equal to the energy normalized by the Fermi energy ε_F. The number of the Landau levels below ε_F is equal to s at $x = s$.

24. Derivation of the oscillatory behavior in a 2D model.

The energy level of each Landau level is given by $\hbar\omega_c(n+1/2)$, where n = 0, 1, 2, ….. Each on of the Landau level is degenerate and contains ρB states. We now consider several cases.

(A) The n = 0, 1, 2, …, s-1 states are occupied. $n = s$ state is empty.

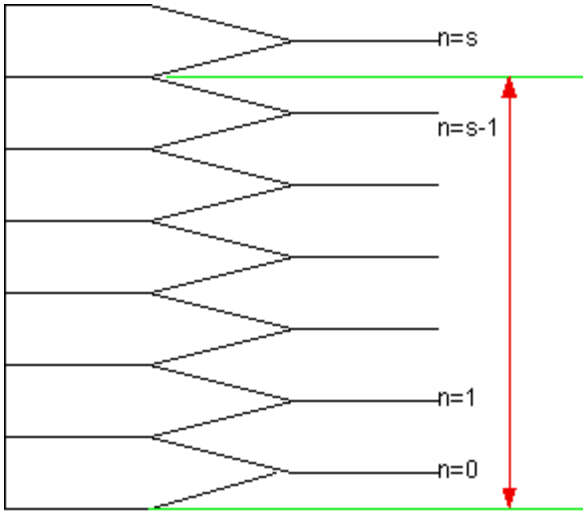

Fig.26 $\varepsilon_F = \hbar\omega_c s$. $N = \rho B s$.

The total energy is constant,

$$U = U_0 = \sum_{n=0}^{s-1} \rho B(n+\frac{1}{2})\hbar\omega_c = \hbar\omega_c \rho B[\frac{1}{2}s(s-1)+\frac{1}{2}s] = \hbar\omega_c \rho B \frac{1}{2}s^2 = \frac{1}{2}\varepsilon_F N. \quad (59)$$

(B) The case where the *n* = *s* state is not filled.

We now consider the case when $\hbar\omega_c$ decreases. This corresponds to the decrease of B.

(i) $\varepsilon < \hbar\omega_c / 2$, where ε is the energy difference defined by the figure below.

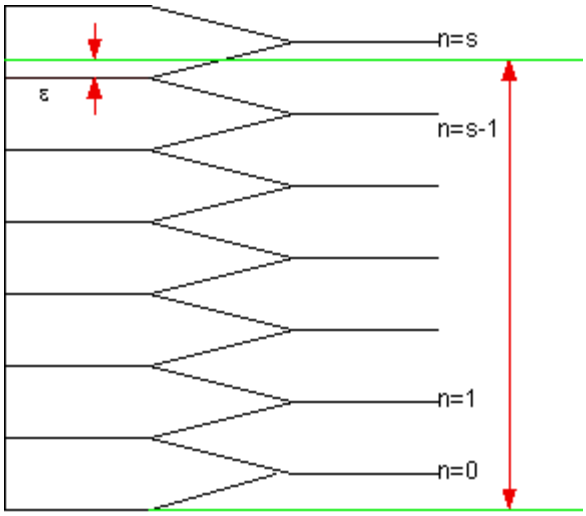

Fig.37

(ii) $\hbar\omega_c / 2 < \varepsilon < \hbar\omega_c$

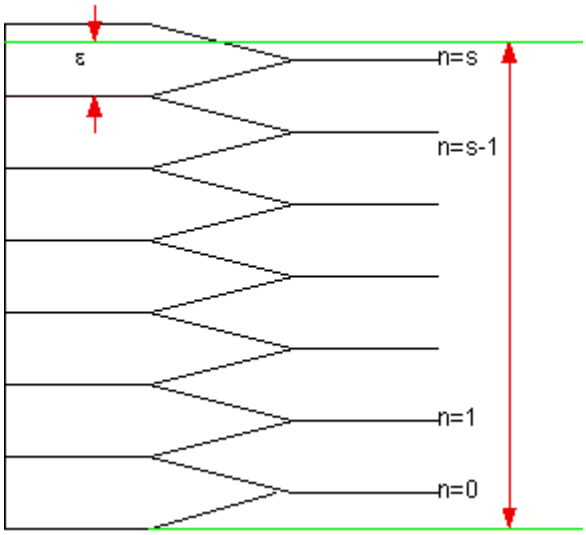

Fig.38 $\varepsilon_F = s\hbar\omega_c + \varepsilon$, with $0 < \varepsilon < \hbar\omega_c$.

The n = 0, 1, 2, …, (s-1) levels are occupied and the $n = s$ level is not filled. The total number of electrons is N. The energy due to the partially occupied $n = s$ state is $(N - \rho Bs)\hbar\omega_c(s + \frac{1}{2})$. Then the total energy is

$$U - U_0 = \sum_{n=0}^{s-1} \rho B(n + \frac{1}{2})\hbar\omega_c - \frac{1}{2}\varepsilon_F N + (N - \rho Bs)\hbar\omega_c(s + \frac{1}{2})$$
$$= \hbar\omega_c \rho B \frac{1}{2}s^2 - \frac{1}{2}\varepsilon_F N + (N - \rho Bs)\hbar\omega_c(s + \frac{1}{2}) \quad (60)$$

,

where

$$\rho Bs < N < \rho B(s+1), \quad \text{and} \quad s\hbar\omega_c < \varepsilon_F = (s+1)\hbar\omega_c.$$

Here we introduce λ as

$$\lambda = N - \rho Bs.$$

The parameter λ satisfies the inequality

$$0 < \lambda < \rho B,$$

for $\frac{\rho s}{N} < \frac{1}{B} < \frac{\rho(s+1)}{N}$. The parameter λ denotes the number of electrons partially occupied in the $n = s$ state

The parameter $\mu = \rho Bs$ is the total number of electrons occupied in the n = 0, 1, 2,…, s-1 states for $\frac{\rho s}{N} < \frac{1}{B} < \frac{\rho(s+1)}{N}$.

(iii) The n = 0, 1, 2, …, s states are occupied. $n = s+1$ state is empty.

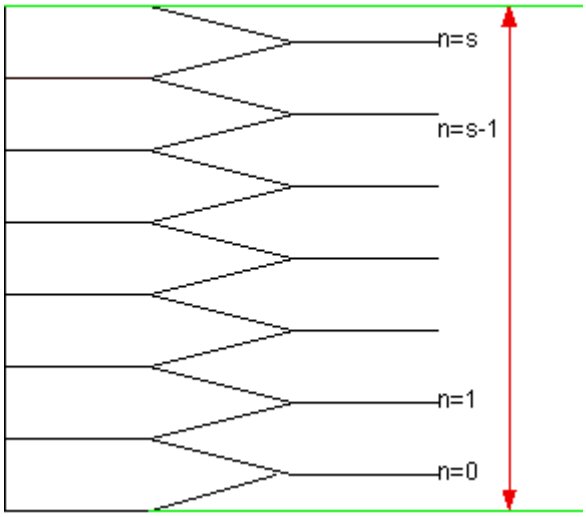

Fig.39

In this case we have

$$\varepsilon_F = \hbar\omega_c(s+1).$$

$$N = \rho B(s+1).$$

$$U = U_0 = \sum_{n=0}^{s} \rho B(n+\frac{1}{2})\hbar\omega_c = \hbar\omega_c \rho B[\frac{1}{2}s(s+1)+\frac{1}{2}(s+1)]$$

$$= \hbar\omega_c \rho B \frac{1}{2}(s+1)^2 = \frac{1}{2}\varepsilon_F N$$

25. Total energy vs *B*

We now discuss the total energy as a function of B.

The total energy has a local minimum at $B = \frac{N(s+\frac{1}{2})}{\rho s(s+1)}$.

((**Proof**))
Since

$$\hbar\omega_c = \frac{\hbar eB}{m_c c} = 2(\frac{e\hbar}{2m_c c})B = 2\mu_B B,$$

the total energy is expressed by

$$U - U_0 = \hbar\omega_c \rho B \frac{1}{2} s^2 - \frac{1}{2}\varepsilon_F N + (N - \rho B s)\hbar\omega_c (s + \frac{1}{2})$$

$$= \mu_B \rho B^2 s^2 - \frac{1}{2}\varepsilon_F N + \mu_B B N(2s+1) - \mu_B \rho B^2 s(2s+1)$$

$$= -\frac{1}{2}\varepsilon_F N + \mu_B B N(2s+1) - \mu_B \rho B^2 s(s+1) = f(B)$$

$$f'(B) = \mu_B N(2s+1) - 2\mu_B \rho B s(s+1) = 0 .$$

Then $f(B)$ has a local maximum at $B = \dfrac{N(s+\frac{1}{2})}{\rho s(s+1)}$,

or

$$\frac{1}{B} = \frac{\rho}{N}\frac{s(s+1)}{s+\frac{1}{2}} .$$

We also show that the total energy $f(B)$ becomes zero at

$$\frac{1}{B} = \frac{s\rho}{N} \text{ and } \frac{1}{B} = \frac{(s+1)\rho}{N} .$$

((**Proof**))
We note that U - U_0=0 at

$$\varepsilon_F = \hbar\omega_c s , \quad \text{and} \quad N = \rho B s .$$

Then

$$\varepsilon_F = \hbar\omega_c s = \frac{e\hbar s}{m_c c} B = \frac{e\hbar}{m_c c} sB = 2\mu_B \frac{N}{\rho} .$$

$$f(B) = -\mu_B \frac{N^2}{\rho} + \mu_B B N(2s+1) - \mu_B \rho B^2 s(s+1) ,$$

or

$$f(B) = -\frac{\mu_B}{\rho}[\rho^2 B^2 s(s+1) - N\rho B(2s+1) + N^2] ,$$

or

$$f(B) = -\mu_B \rho[B^2 s(s+1) - \frac{N}{\rho} B(2s+1) + \frac{N^2}{\rho^2}]$$
$$= -\mu_B \rho(sB - \frac{N}{\rho})[(s+1)B - \frac{N}{\rho}] \quad .$$

The solution of $f(B) = 0$ is

$$\frac{1}{B} = \frac{s\rho}{N} \text{ and } \frac{1}{B} = \frac{(s+1)\rho}{N}.$$

23. Magnetization *M* vs *B*

The magnetization M is given by

$$M = -\frac{\partial U}{\partial B} = -\frac{\partial B}{\partial x}\frac{\partial U}{\partial x} = x^2 \frac{\partial U}{\partial x} = x^2 \frac{N^2 \mu_B}{\rho}\frac{\partial F}{\partial x}, \tag{61}$$

where

$$x = \frac{1}{B},$$

$$F = -s(s+1)\frac{\rho^2}{N^2}\frac{1}{x^2} + \frac{\rho}{N}(2s+1)\frac{1}{x} - 1,$$

$$\frac{\partial F}{\partial x} = 2s(s+1)\frac{\rho^2}{N^2}\frac{1}{x^3} - \frac{\rho}{N}(2s+1)\frac{1}{x^2},$$

$$M = x^2 \frac{N^2 \mu_B}{\rho}\frac{\partial F}{\partial x} = \frac{N^2 \mu_B}{\rho}[2s(s+1)\frac{\rho^2}{N^2}\frac{1}{x} - \frac{\rho}{N}(2s+1)].$$

$M = 0$ at

$$x = \frac{2s(s+1)}{2s+1}\frac{\rho}{N}.$$

26. Mathematica

In this numerical calculation we use $n = 10$, $\mu_B = 1$, and $\rho = 1.$ for simplicity.

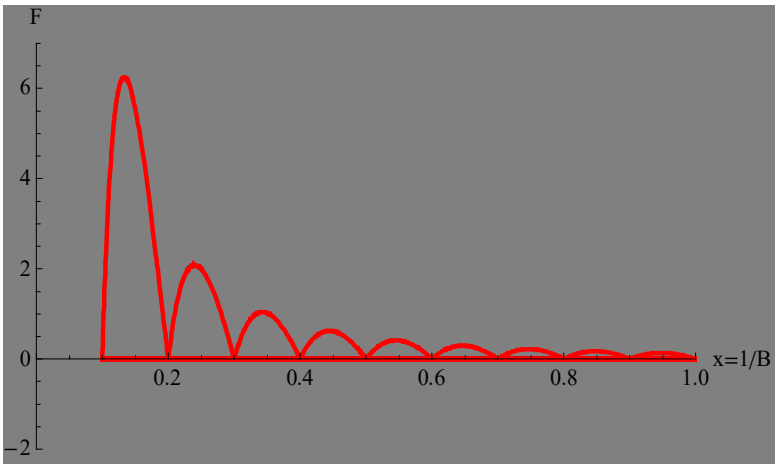

Fig.40 The plot of U-U_0 vs $1/B$ (the detail).

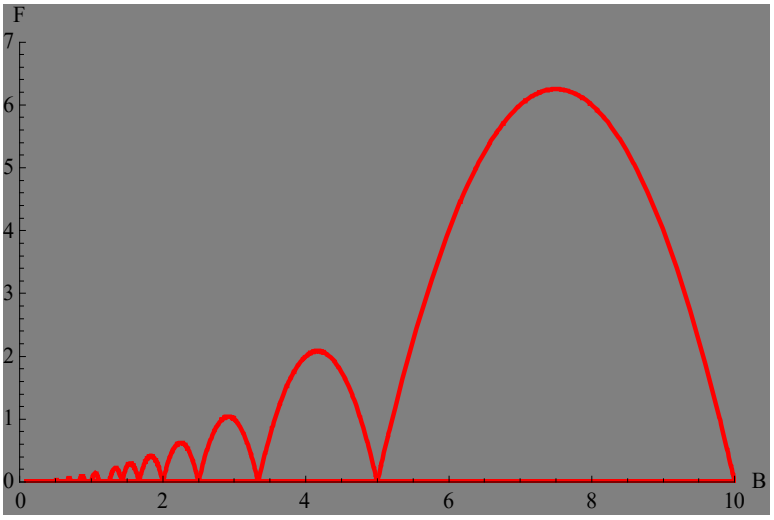

Fig.41 Plot of U-U_0 vs B.

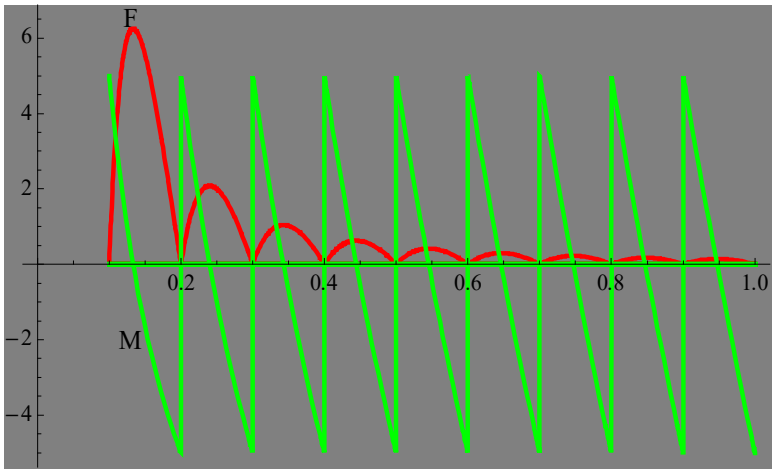

Fig.42 Plot of U-U_0 and M as a function of $1/B$.

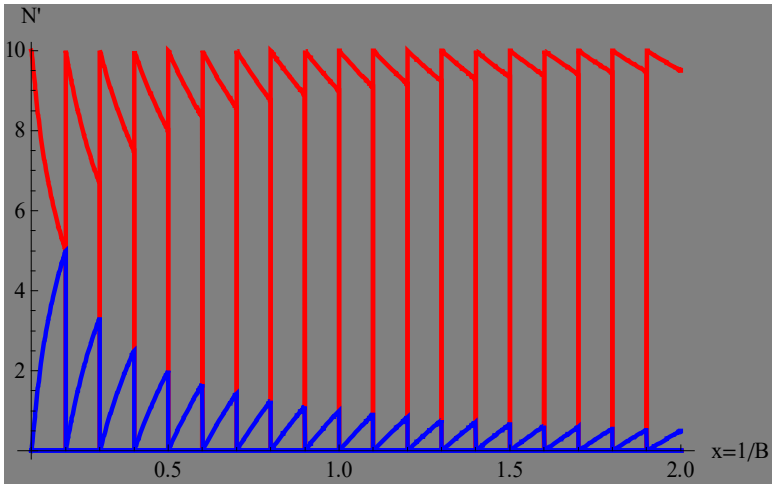

Fig. 43 Plot of μ vs $1/B$ (red) and λ vs $1/B$ (blue).

27. Conclusion

The physics on the dHvA effect of metals (in particular, bismuth) has been presented with the aid of Mathematica 5.2.

REFERENCES

1. L. Landau, Z. Phys. **64**, 629 (1930).
2. L. Onsager, Phil. Mag. **43**, 1006 (1952).
3. D. Shoenberg, Proc. Roy. Soc. A **170**, 341 (1939).
4. M.H. Cohen, Phys. Rev. **121**, 387 (1962).
5. R.N. Brown, J.G. Mavroides, and B. Lax, Phys. Rev. **129**, 2055 (1963).
6. G.E. Smith, G.A. Baraff, and J.M. Rowell, Phys. Rev. B **135**, A1118 (1964).
7. R.N. Bhargrava, Phys. Rev. **156**, 785 (1967).
8. S. Takano and H. Kawamura, J. Phys. Soc. Jpn. **28**, 348 (1970).
9. M. Suzuki; Ph.D. Thesis at the University of Tokyo (1977).
10. M. Suzuki, H. Suematsu, and S. Tanuma, J. Phys. Soc. Jpn.**43**, 499 (1977).

11. I.M. Lifshitz and A.M. Kosevich, Sov. Phys. JETP **2**, 636 (1956).
12. A.B. Pippard, *Dynamics of conduction electrons*. (Gordon and Breach, New York, 1965).
13. A.A. Abrikosov, Solid State Physics Supplement 12, *Introduction to the theory of normal metals,* (Academic Press, New York, 1972).
14. D. Shoenberg, *Magnetic oscillations in metals*. (Cambridge University Press, London, 1984).
15. C. Kittel, *Introduction to Solid State Physics*, Sixth edition, (John Wiley and Sons Inc., New York, 1986).
16. R.G. Chambers
17. A.B. Pippard, *The Dynamics of Conduction Electrons*, Gordon and Breach (New York, 1965).
18. A.B. Pippard, *Magnetoresistance in Metals* (Cambridge University Press, 1989).
19. J. Singleton, *Band Theory and Electron Properties of Solids* (Oxford University Press, 2001).

APPENDIX

APPENDIX-1

de Haas van Alphen effect

```
Clear["Global`*"];
U = -1/2 s (s + 1) μB ρ B^2 + N1 (s + 1/2) μB B - 1/2 N1 EF /.
   (EF → μB N1/ρ); eq1 = D[U, B]; Solve[eq1 == 0, B];

U1[x_, s_] = U /. B → 1/x // Simplify;

U2 = U1[x, s] x^2 ρ / N1^2 // PowerExpand // Simplify;

Solve[U2 == 0, x] // Simplify;

max1 = U1[x, s] /. {x → s (1 + s) ρ / (N1 (s + 1/2))} // Simplify;

rule1 = {N1 → 10, ρ → 1, μB → 1};

H[x_, s_, N1_, ρ_] :=
 UnitStep[x - s ρ/N1] - UnitStep[x - (1 + s) ρ/N1];

U2 = U1[x, s] H[x, s, N1, ρ]; U4 = U2 /. {x → 1 / y};

M = x^2 D[U2, x] // Simplify; NN1 = N1 - ρ B s;

NN2[x_, s_] = NN1 /. B → 1 / x // Simplify;

NN3 =
 NN2[x, s] (UnitStep[x - s ρ/N1] - UnitStep[x - (1 + s) ρ/N1]);

NN4 = s ρ/x (UnitStep[x - s ρ/N1] - UnitStep[x - (1 + s) ρ/N1]);
```

Free energy as a function of x = 1/B

```
p11 = Plot[Evaluate[Table[U2 /. rule1, {s, 0, 20}]],
  {x, 0.1, 1},
  PlotStyle → Table[{Hue[0. i], Thick}, {i, 0, 10}],
  PlotRange → {{0, 1}, {-2, 7}}, Background → Gray,
  AxesLabel → {"x=1/B", "F"}]
```

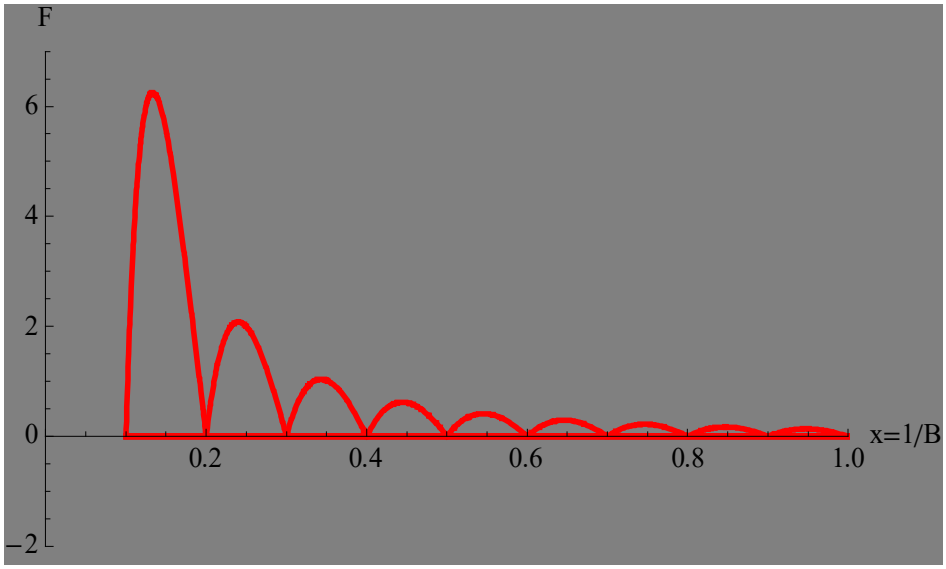


```
p111 = Plot[Evaluate[Table[U4 /. rule1, {s, 0, 20}]],
  {y, 0.1, 10},
  PlotStyle → Table[{Red, Thick}, {i, 0, 10}],
  PlotRange → {{0, 10}, {0, 7}}, Background → Gray,
  AxesLabel → {"B", "F"}]
```

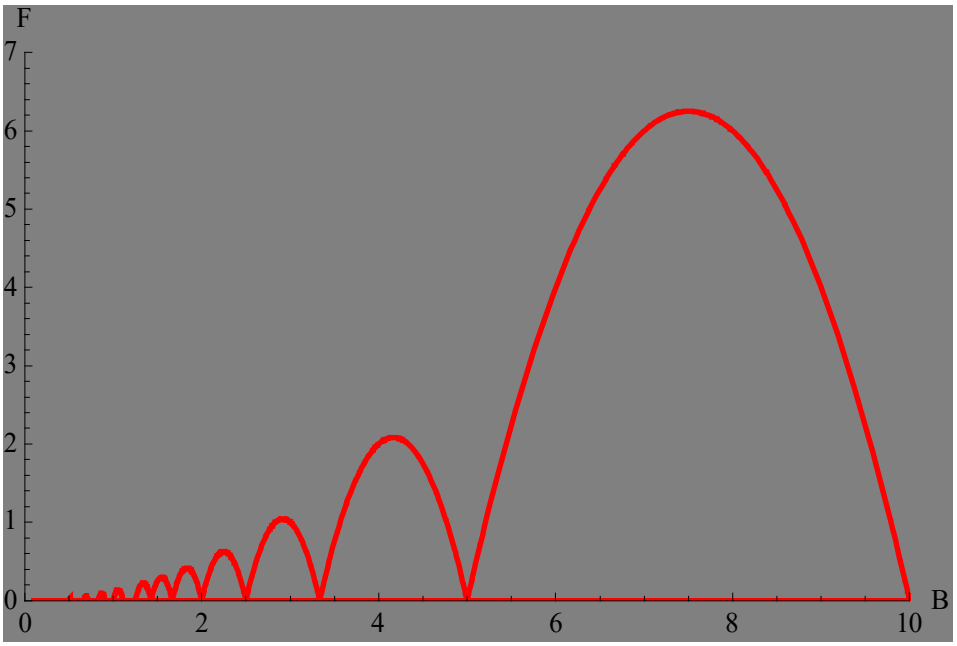

Magnetization as a function of 1/B

```
p11 = Plot[Evaluate[Table[U2 /. rule1, {s, 0, 20}]],
   {x, 0.1, 1},
   PlotStyle → Table[{Hue[0. i], Thick}, {i, 0, 10}],
   PlotRange → {{0, 1}, {-2, 7}}, Background → Gray];
p12 = Plot[Evaluate[Table[M /. rule1, {s, 0, 20}]],
   {x, 0.1, 1},
   PlotStyle → Table[{Green, Thick}, {i, 0, 20}],
   PlotRange → {{0, 1}, {-7, 7}}, Background → Gray,
   PlotPoints → 200, Exclusions → None];
g1 =
 Graphics[
   {Text[Style["F", Black, 12], {0.13, 6.5}],
    Text[Style["M", Black, 12], {0.13, -2}]}];
Show[p11, p12, g1, PlotRange → All]
```

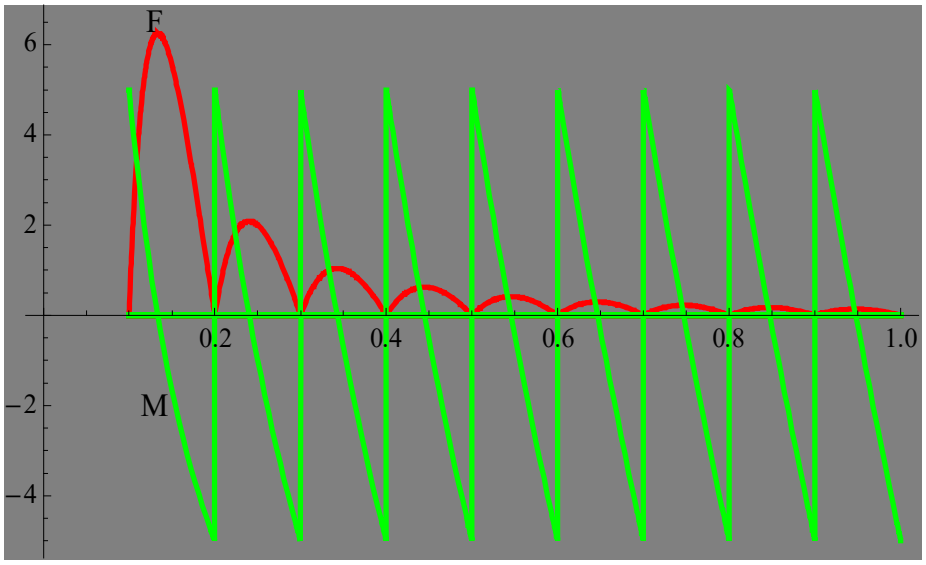


```
b11 = Plot[Evaluate[Table[NN3 /. rule1, {s, 0, 20}]],
   {x, 0.1, 2},
   PlotStyle → Table[{Blue, Thick}, {i, 0, 20}],
   Background → Gray, AxesLabel → {"x=1/B", "N'"},
   Exclusions → None];
b22 = Plot[Evaluate[Table[NN4 /. rule1, {s, 0, 20}]],
   {x, 0.1, 2},
   PlotStyle → Table[{Red, Thick}, {i, 0, 20}],
   Background → Gray, AxesLabel → {"x=1/B", "N'"},
   Exclusions → None];
Show[b22, b11]
```

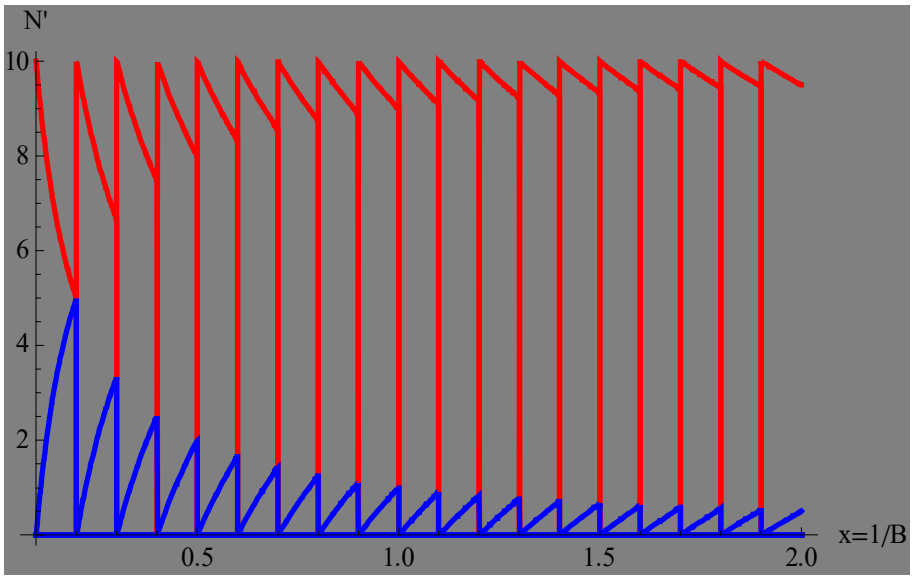

APPENDIX 2 How to draw the dHvA tubes using Mathematica

```
Clear["Global`*"];
dHvA[A1_, E1_] := Module[{N1}, N1 = (2 E1/A1 - 1)/2; r[n1_] := Sqrt[(2 n1 + 1) A1];
  kz1[n2_] := Sqrt[2 E1 - (2 n2 + 1) A1];
  f1 =
   Graphics3D[{Green, Opacity[0.25], Table[Cylinder[{{0, 0, -kz1[n]}, {0, 0, kz1[n]}}, r[n]],
      {n, 0, N1}]}, ViewPoint → {1, 1, 0.4}, Boxed → False];
  f2 = Graphics3D[{{Red, Thick, Arrow[{{0, 0, Sqrt[2 E1]}, {0, 0, 1.6 Sqrt[2 E1]}}]},
     Text[Style["B" , Black, 15], {0, 0, 1.2 Sqrt[2 E1]}],
     Text[Style["E=" <> ToString[E1], Black, 15], {1.5 Sqrt[2 E1], 0, 0}],
     Text[Style["ħω_c=" <> ToString[A1], Black, 15], {1.5 Sqrt[2 E1], 0, -1}]}];
  Show[f1, f2, PlotRange → All]];
pt2 = Evaluate[Table[dHvA[A1, 12], {A1, 3, 8, 1}]];
Show[GraphicsGrid[Partition[pt2, 3]]]
```

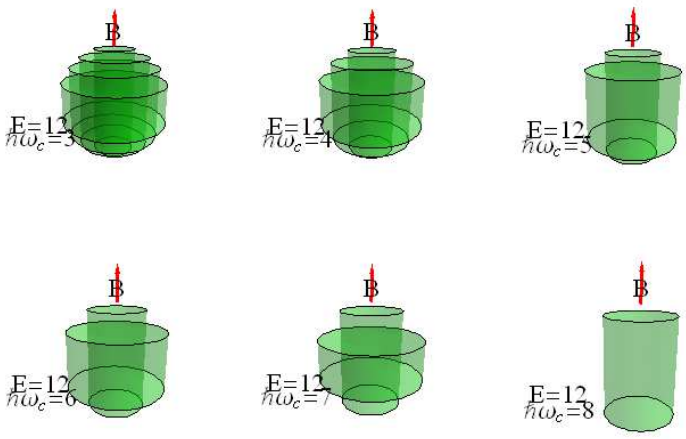

APPENDIX-III

Units related to this section

$[e^2]$ = erg cm

[erg]= $[G^2.cm^3]$

[emu] = [erg/G]

Since

$[e^2]$ = erg cm = G^2cm^4,

we have

[e] = G cm^2

We note that

$$[\text{emu}]=\frac{erg}{G}=\frac{G^2\cdot cm^3}{G}=G\cdot cm^3$$

---

(1) The units of $\frac{e}{\hbar c}$

$$[\frac{e}{\hbar c}]=\frac{1}{G\cdot cm^2}$$

(2) The units of ρ

$$[\rho(=\frac{eL^2}{2\pi\hbar c})]=\frac{1}{G}$$

(3) The units of the length l

$$[l^2(=\frac{c\hbar}{eB})]=\text{cm}^2.$$

(4) The units of ω_c

$$[\omega_c(=\frac{eB}{m_c c})]=\frac{G^2\cdot cm^2}{erg(s^2/cm^2)(cm/s)}=\frac{G^2\cdot cm^3}{erg\cdot s}=\frac{G^2\cdot cm^3}{G^2\cdot cm^3\cdot s}=\frac{1}{s}$$